Phys. Lett. B 858 (2024) 139044

Contents lists available at ScienceDirect

Physics Letters B

journal homepage: www.elsevier.com/locate/physletb

Letter

Measurement of the polarizations of prompt and non-prompt J/ψ and ψ(2S) mesons produced in pp collisions at $\sqrt{s} = 13\,\text{TeV}$

The CMS Collaboration ⋆

CERN, Geneva, Switzerland

ARTICLE INFO

Editor: M. Doser

Keywords:
CMS
Quarkonium production
Quarkonium polarization

ABSTRACT

The polarizations of prompt and non-prompt J/ψ and ψ(2S) mesons are measured in proton-proton collisions at $\sqrt{s} = 13\,\text{TeV}$, using data samples collected by the CMS experiment in 2017 and 2018, corresponding to a total integrated luminosity of $103.3\,\text{fb}^{-1}$. Based on the analysis of the dimuon decay angular distributions in the helicity frame, the polar anisotropy, λ_ϑ, is measured as a function of the transverse momentum, p_T, of the charmonium states, in the 25–120 and 20–100 GeV ranges for the J/ψ and ψ(2S), respectively. The non-prompt polarizations agree with predictions based on the hypothesis that, for $p_\text{T} \gtrsim 25\,\text{GeV}$, the non-prompt J/ψ and ψ(2S) are predominantly produced in two-body B meson decays. The prompt results clearly exclude strong transverse polarizations, even for p_T exceeding 30 times the J/ψ mass, where λ_ϑ tends to an asymptotic value around 0.3. Taken together with previous measurements, by CMS and LHCb at $\sqrt{s} = 7\,\text{TeV}$, the prompt polarizations show a significant variation with p_T, at low p_T.

1. Introduction

Charmonium and bottomonium production provides an ideal case study for the understanding of hadron formation in quantum chromodynamics (QCD) [1,2]. Its theoretical description is based on the generally agreed assumption that the charm and beauty quarks (the heaviest ones capable of forming bound states) are heavy enough to allow the factorization of short- and long-distance effects. Within the non-relativistic QCD (NRQCD) framework [3], in particular, perturbative QCD computations provide the production cross sections of the $\text{Q}\overline{\text{Q}}$ heavy-quark pair (the “short-distance coefficients”, SDCs), while the non-perturbative evolution of the $\text{Q}\overline{\text{Q}}$ state to the observed meson (hadronization) is described by phenomenological parameters (the “long-distance matrix elements”, LDMEs), determined from fits to experimental data. Other theoretical approaches have been considered, such as the color-singlet model (CSM) [4,5] and the color-evaporation model (CEM) [6,7]. These theoretical models differ in the choice and classification of the allowed pre-resonance states. The NRQCD approach foresees the contribution of all possible spin, S, orbital angular momentum, L, total angular momentum, J, and color ($c = 1$ or 8) configurations, $\text{Q}\overline{\text{Q}}(^{2S+1}L_J^{[c]})$, organized in an expansion in powers of the relative $\text{Q}\overline{\text{Q}}$ velocity so that only a small number of leading and sub-leading terms remain quantitatively important. Instead, the CSM considers that the final-state hadron can only result from a color-neutral (singlet) pre-resonance state having the same quantum numbers, while the CEM is built upon the assumption that the probability of forming a specific quarkonium state is independent of its kinematics and spin, as well as of the production process.

According to the perturbative calculations of the relevant partonic processes, the observable transverse momentum (p_T) distributions of the produced quarkonium meson depend significantly on the angular momentum quantum state of the unobservable $\text{Q}\overline{\text{Q}}$ pre-resonance. Moreover, the contributing short-distance processes (one, few, or many, depending on the model) are scaled by long-distance weights that further depend on the angular momentum quantum numbers of each pre-resonance. Therefore, by foreseeing different pre-resonance mixtures, the CSM, CEM, and NRQCD predict, in general, different distributions for p_T and other kinematic variables. The polarization of the quarkonium state is, however, the observable that most directly reflects the mixture of S, L, J configurations (and polarizations) of the contributing pre-resonance states, as it can be understood independently of any perturbative calculation. Consequently, polarization measurements provide particularly straightforward information regarding the details of the hadronization models. The polarizations of five vector ($J^{PC} = 1^{--}$) quarkonia, J/ψ, ψ(2S), ϒ(1S), ϒ(2S) and ϒ(3S), have been measured, as functions of p_T, at the Fermilab Tevatron [8,9] and the CERN LHC [10–14]. These measurements have been considered in several phe-

⋆ *E-mail address:* cms-publication-committee-chair@cern.ch.

https://doi.org/10.1016/j.physletb.2024.139044
Received 20 June 2024; Received in revised form 29 August 2024; Accepted 24 September 2024
Available online 30 September 2024

nomenological studies, including analyses based on the NRQCD [15–21] and CEM [22] approaches. Measurements of inclusive J/ψ polarizations, where the contribution from decays of b hadrons is not subtracted, have been reported by the PHENIX, STAR, and ALICE Collaborations [23–25].

Within the precision of the previous CMS measurements [10,26], no significant deviation is seen with respect to the "unpolarized scenario", where the directly (i.e., excluding feed-down decays) produced J/ψ mesons have zero and p_T-independent polarization [27]. The straightforward interpretation of that scenario would be that J/ψ production is dominated by the (unpolarized) ${}^1S_0^{[8]}$ color-octet state, an option not naturally foreseen by NRQCD, where the LDMEs of the strongly polarized ${}^3S_1^{[8]}$ and ${}^3P_J^{[8]}$ octet contributions and of the ${}^1S_0^{[8]}$ term are expected to have similar magnitudes, leading to a significant p_T dependence of the polarization. In principle, one might think that sufficiently precise p_T-differential cross section measurements would be able to discriminate between those two scenarios, one where the ${}^1S_0^{[8]}$ term dominates and the other also including significant ${}^3S_1^{[8]}$ and ${}^3P_J^{[8]}$ contributions. In practice, however, this is not the case, because of two facts [28]. First, an accidental degeneracy makes the shape of a certain combination of the ${}^3S_1^{[8]}$ and ${}^3P_J^{[8]}$ p_T distributions indistinguishable from the ${}^1S_0^{[8]}$ one. Second, both the shape of that combination and the shape of the ${}^1S_0^{[8]}$ term are very similar to the measured J/ψ p_T distribution, indicating that reality is critically close to the degeneracy condition. Therefore, the observed p_T distribution has a weak resolving power on the participating processes. In fact, fits trying to determine the relative process contributions, i.e. the LDMEs, using only the measured differential cross sections as constraints can lead to ambiguous results [19]. The polarization measurement provides a completely independent and sensitive source of information: any ${}^3S_1^{[8]} + {}^3P_J^{[8]}$ combination leads to a recognizable p_T-dependent polarization, changing monotonically from longitudinal to transverse as p_T increases. Therefore, a sufficiently precise polarization measurement, performed over a wide-enough p_T range, should be able to reveal the relative contributions of the differently polarized color octet terms.

This Letter reports a new measurement of the prompt J/ψ and ψ(2S) polarizations, in proton-proton (pp) collisions at a center-of-mass energy of 13 TeV, based on data collected by the CMS experiment in 2017 and 2018, corresponding to a total integrated luminosity of 103.3 fb^{-1}. This event sample is much larger than the one collected in 2011, at 7 TeV, which was used for the previous measurement [10]. The results are sufficiently accurate to provide the sensitivity needed to evaluate the relative proportions of the three color octet channels. We also present the first LHC measurement of the polarizations of non-prompt J/ψ and ψ(2S) mesons, predominantly produced in decays of B mesons, with a small contribution from decays of other b hadrons. This result provides an independent probe of the charmonium formation mechanism and of its composition in terms of singlet and octet contributions. Besides the directly produced component, the prompt J/ψ yield includes fractions from "feed-down decays" of heavier charmonium states: around 8% from ψ(2S) decays and 25% from χ_c decays [29].

The average polarizations of $J^{PC} = 1^{--}$ quarkonia are usually determined by measuring the angular distributions of the positively charged muons emitted in the decay of the mesons, which have the general observable form [30,31]

$$W(\cos\vartheta, \varphi \mid \vec{\lambda}) = \frac{3}{4\pi(3+\lambda_\vartheta)}\left(1 + \lambda_\vartheta \cos^2\vartheta + \lambda_\varphi \sin^2\vartheta \cos 2\varphi + \lambda_{\vartheta\varphi} \sin 2\vartheta \cos\varphi\right), \tag{1}$$

where ϑ and φ are the polar and azimuthal angles of the muon in the quarkonium rest frame with respect to, respectively, a suitably defined polarization axis z and the plane containing the momenta of the colliding beams and of the quarkonium [32]. The shape of the decay angular distribution is defined by the polarization parameters λ_ϑ, λ_φ, and $\lambda_{\vartheta\varphi}$. Depending on the chosen polarization frame, not all three parameters contain equally significant and/or independent physical information, as is extensively discussed in Ref. [32]. In particular, in a domain where the laboratory momentum is always much larger than the particle mass M, it can be safely assumed (as seen, for example, in Drell–Yan and Z boson production measurements in the limit of very high p_T/M [33,34]) that azimuthal anisotropies become negligible in the center-of-mass helicity frame (HX), where the z axis coincides with the particle momentum direction in the center-of-mass frame of the colliding hadrons [32]. Moreover, at mid-rapidity and in the limit of high p_T, relevant for the present measurement, the shape of the muon pair acceptance as a function of $\cos\vartheta_{HX}$ becomes essentially independent of φ_{HX} so that Eq. (1) can be integrated over the azimuthal decay angle and the analysis can focus on the simpler one-parameter distribution

$$W(\cos\vartheta_{HX}) \propto 1 + \lambda_\vartheta^{HX} \cos^2\vartheta_{HX}, \tag{2}$$

without the risk of being biased by neglected correlation effects. In this phase space window (high p_T and mid-rapidity) the perpendicular helicity frame [35] is indistinguishable from the HX frame. On the other hand, the Collins–Soper (CS) frame [36] is unsuitable because it is not possible to integrate the $\cos\vartheta_{CS}$ vs. φ_{CS} acceptance map over the azimuthal decay angle without including zero-acceptance domains, so that a two-dimensional analysis becomes necessary [32].

2. Apparatus, event samples, and selection criteria

The CMS apparatus is a multipurpose detector [37] designed to trigger on and identify electrons, muons, photons, and (charged and neutral) hadrons [38–40]. A superconducting solenoid of 6 m internal diameter provides a magnetic field of 3.8 T. Within the solenoid volume are the silicon pixel and strip tracker, a crystal electromagnetic calorimeter, and a brass and scintillator hadron calorimeter. Muons are measured in gas-ionization detectors embedded in the steel flux-return yoke outside the solenoid. Events of interest are selected using a two-tiered trigger system. The first level, composed of custom hardware processors, uses information from the calorimeters and muon detectors to select events at a rate of 100 kHz within a fixed latency of 4 μs [41]. The second level, consisting of a farm of processors running a faster version of the full event reconstruction software, reduces the rate to around 1 kHz, before data storage [42].

The event samples used in the analysis were collected in 2017 and 2018, with integrated luminosities of 42.0 and 61.3 fb^{-1}, respectively [43,44]. The events were selected by two dimuon triggers, requiring an opposite-sign muon pair with the invariant mass in the ranges $2.9 < M < 3.33$ GeV for the J/ψ case and 3.35–4.05 GeV for the ψ(2S) case. The distance of closest approach between the two muons must be smaller than 0.5 cm and a fit of the positions and momenta of the two muons to a common vertex ("dimuon vertex fit") must have a χ^2 probability larger than 0.5%. In addition, to reduce the trigger rate, the dimuon p_T must be larger than 24.9 and 17.9 GeV for the J/ψ and ψ(2S) events, respectively. No explicit p_T requirement was imposed on the individual muons at the trigger level. The dimuon rapidity is restricted to $|y| < 1.25$, where the muon momentum is measured with the best resolution.

The reconstructed data were processed ensuring that both reconstructed muons must match, in pseudorapidity (η) and azimuthal angle, those that triggered the detector readout. Both muon tracks must have more than five hits in the silicon tracker, at least one of them being in a pixel detector layer. They must also fulfill other ("soft-muon") identification requirements [39], which include the (loose) matching between the track reconstructed in the silicon tracker and the one reconstructed in the muon detectors. The two muons of the selected events must each have $p_T > 5.6$ GeV, $|\eta| < 1.4$, and a dimuon vertex fit χ^2 probability larger than 1%. The single muon p_T requirement ensures that all selected muons are in the plateau region of the detection efficiency, so that the efficiency variations are smaller than 5%. The polarizations are measured in the p_T ranges 25–120 GeV (in 19 bins) and 20–100 GeV (in 8 bins) for the J/ψ and ψ(2S) mesons, respectively. The results are

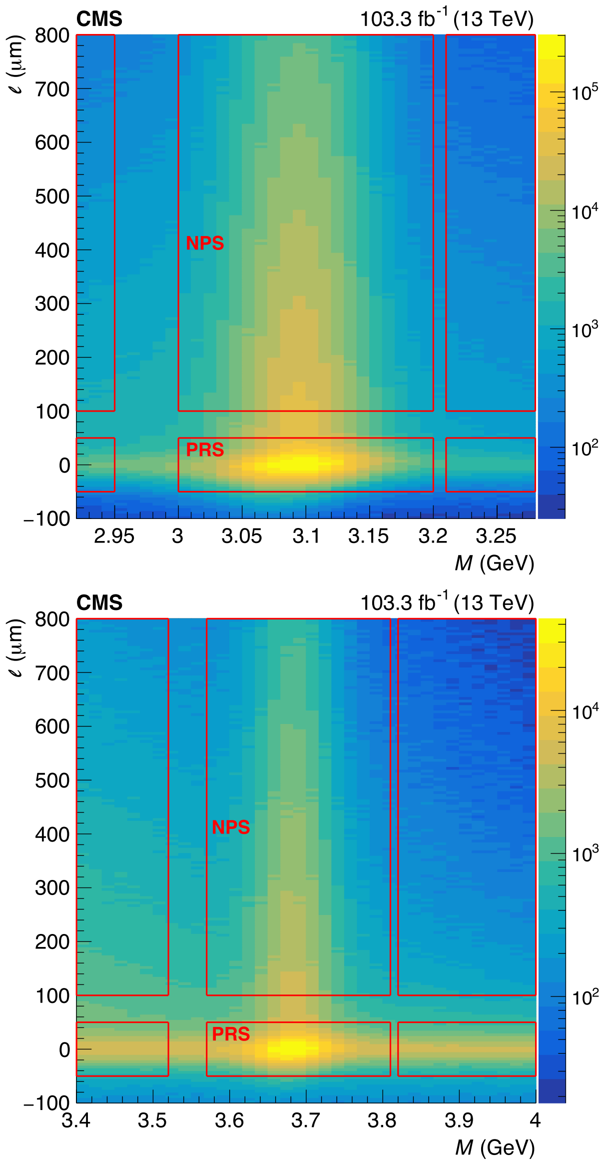

Fig. 1. Measured dimuon decay length vs. mass distributions for the J/ψ (top) and ψ(2S) (bottom) samples, showing the rectangular regions used in the analysis. The prompt and non-prompt signal regions are labeled PRS and NPS, respectively, while the remaining regions are non-signal (sideband) regions.

obtained in the dimuon rapidity window $|y| < 1.2$. The dimuon mass distributions, studied in the 2.92–3.28 and 3.4–4.0 GeV ranges for the J/ψ and ψ(2S) cases, respectively, provide the information needed to separate the signal contributions (dimuons from the J/ψ and ψ(2S) decays) from the underlying continuum background, composed of muon pairs resulting from other processes, such as decays of heavy-flavor hadrons.

For each of the two charmonium states and each of the p_T bins, the $|\cos\vartheta_{HX}|$ distributions are measured in six independent event samples, defined by three ranges in the dimuon mass (signal window and two sidebands) and two in the dimuon pseudo-proper decay length (prompt and non-prompt). The six windows are presented in Fig. 1, for the J/ψ and ψ(2S) analyses. The dimuon pseudo-proper decay length [45], abbreviated as "decay length" in the remainder of this Letter, is defined as $\ell = M \vec{L}_{xy} \cdot \vec{p}_T / p_T^2$, where $\vec{L}_{xy}$ is the displacement in the transverse plane between the primary vertex and the dimuon production vertex; it is measured with a resolution around 25 μm. The primary vertex is selected among all reconstructed pp collision vertices in the event as the one closest to the line extrapolating the dimuon momentum back to the beam line and its position is determined by fitting all tracks associated with the vertex other than the two selected muons. In the following, we use the labels PRS ("prompt signal") and NPS ("non-prompt signal") to identify the dimuon mass vs. decay length two-dimensional windows used to measure the prompt ($|\ell| < 50\,\mu$m) and non-prompt ($100 < \ell < 800\,\mu$m) J/ψ (3.0–3.2 GeV) and ψ(2S) (3.57–3.81 GeV) meson polarizations. We also use PR and NP as subscripts to denote the event samples with $|\ell| < 50\,\mu$m and $100 < \ell < 800\,\mu$m, respectively. The J/ψ analysis uses 14.7 M and 10.9 M events in the PRS and NPS windows, respectively; the corresponding numbers for the ψ(2S) analysis are 2.1 M and 1.4 M. The other four windows are mass sidebands used for the subtraction of the continuum dimuon background: 2.92–2.95 and 3.21–3.28 GeV for the J/ψ analysis, and 3.4–3.52 and 3.82–4.0 GeV for the ψ(2S) analysis.

The detection acceptance and efficiency effects are evaluated through detailed Monte Carlo (MC) simulations of the entire data collection and reconstruction chain, from the trigger step to the offline event selection. The events are generated assuming unpolarized production, so that any non-flat trends seen in the reconstructed distributions are caused by the convolution of the detection effects. The J/ψ and ψ(2S) event samples are generated with the PYTHIA 8.240 event generator [46]. The emitted muons undergo final-state radiation, generated through the PHOTOS 3.61 package [47]. The simulation includes effects from multiple pp interactions in the same or nearby bunch crossings, with a multiplicity distribution tuned to match the data. The simulated events are then processed through a detailed simulation of the CMS detector, based on the GEANT4 package [48], using the same trigger and reconstruction algorithms as used to collect and process the data; they also need to pass the same selection criteria. The simulated samples are independently generated for each of the two data-taking years and several validation checks were performed to ensure that they reliably reproduce the running conditions of the experiment during those periods. The polarization measurement is insensitive to the acceptance and efficiency magnitudes; only their variation with $|\cos\vartheta_{HX}|$, in each p_T bin, is relevant. The detection acceptance and efficiency is approximately flat with $\cos\vartheta_{HX}$, except close to the edge of the covered $|\cos\vartheta_{HX}|$ window, where it drops. The coverage in $|\cos\vartheta_{HX}|$ is determined by the $p_T > 5.6$ GeV requirement on the individual muons and increases from $|\cos\vartheta_{HX}| < 0.5$ to $|\cos\vartheta_{HX}| < 0.9$, between the lowest and highest dimuon p_T bins of the analysis.

3. Dimuon mass and decay length analysis

3.1. Analysis overview

The polarizations measured in this analysis are reported using the polar anisotropy parameter λ_ϑ^{HX}, extracted by fitting the $|\cos\vartheta_{HX}|$ distributions with Eq. (2); in the following, for simplicity, we drop the superscript HX. We start by describing the measurement of the polarizations of the non-prompt J/ψ and ψ(2S) mesons. While a small fraction of those mesons is produced in decays of b baryons, they are predominantly the daughters of B mesons and, hence, we denote them as ψ_B. The dimuons contributing to the $|\cos\vartheta_{HX}|$ distribution in the non-prompt signal mass region for a given p_T bin, $\mathrm{NPS}(|\cos\vartheta_{HX}|, p_T)$, come either from decays of ψ_B mesons or from non-prompt continuum background processes, C_{NP},

$$\begin{aligned}\mathrm{NPS}(|\cos\vartheta_{HX}|, p_T) &= f^{\mathrm{NPS}}_{\psi_B}(p_T)\,\psi_B(|\cos\vartheta_{HX}|, p_T)\\ &+ f^{\mathrm{NPS}}_{C_{NP}}(p_T)\,C_{NP}(|\cos\vartheta_{HX}|, p_T),\end{aligned} \tag{3}$$

with $f^{\mathrm{NPS}}_{\psi_B}(p_T) = 1 - f^{\mathrm{NPS}}_{C_{NP}}(p_T)$.

Similarly, the polarizations of the prompt J/ψ and ψ(2S) mesons, ψ_P, can also be measured, in each p_T bin, using the $|\cos\vartheta_{HX}|$ distributions of the dimuons in the prompt signal region, $\mathrm{PRS}(|\cos\vartheta_{HX}|, p_T)$. However, besides the dimuons from prompt charmonia and from continuum background processes, C_{PR}, the PRS window also includes events from charmonia produced in decays of short-lived B mesons, of $|\ell| < 50\,\mu m$,

$$\mathrm{PRS}(|\cos\vartheta_{HX}|, p_T) = f^{PRS}_{\psi_P}(p_T)\,\psi_P(|\cos\vartheta_{HX}|, p_T) + f^{PRS}_{C_{PR}}(p_T)\,C_{PR}(|\cos\vartheta_{HX}|, p_T) + f^{PRS}_{\psi_B}(p_T)\,\psi_B(|\cos\vartheta_{HX}|, p_T), \quad (4)$$

with $f^{PRS}_{\psi_P}(p_T) = 1 - f^{PRS}_{C_{PR}}(p_T) - f^{PRS}_{\psi_B}(p_T)$.

The fractions of continuum muon pairs in the signal windows, $f^{NPS}_{C_{NP}}$ and $f^{PRS}_{C_{PR}}$, are determined from fits to the dimuon mass distributions, while the fractions of charmonia from B meson decays in the prompt signal window, $f^{PRS}_{\psi_B}$, are obtained by fitting the dimuon decay length distributions, accounting for the existence of non-prompt continuum muon pairs. The continuum dimuons in the PR region include prompt Drell–Yan dimuons and several combinations of muons produced in decays of pions, kaons, D mesons, and B mesons. The remainder of this section explains how the three fractions are measured, for each of the two charmonium states and as functions of p_T, and reports the results, which are then used in the measurement of the polarizations.

3.2. Background fractions in the non-prompt charmonium signal regions

The fits of the non-prompt J/ψ and ψ(2S) dimuon mass distributions, illustrated in the top and bottom panels of Fig. 2, respectively, are conceptually identical except for the functions describing the signal shape. We start with the simpler ψ(2S) case.

The eight dimuon mass distributions (corresponding to the eight ψ(2S) p_T bins) are simultaneously fitted by the sum of two Crystal Ball (CB) functions [49], to describe the ψ(2S) line shape, plus a decreasing exponential function, to describe the underlying continuum background. The two CB functions have common means ($\mu_1 = \mu_2$) and tail parameters n and α, but independent widths (σ_1 and σ_2). A good description of all of the ψ(2S) dimuon mass distributions is obtained with a relatively small number of free shape parameters by constraining their dependence on p_T following studies of the MC event samples validated on the measured data. More specifically, the CB means and their relative proportions are independent of p_T, as is the value of α, while the two widths increase linearly with p_T, with a common slope. The tail parameter n is fixed to 2.5, a value based on studies of simulated events; given the strong correlation between n and α, it is reasonable to leave only one of them as a free parameter in the fit. Fig. 2 (bottom) shows the measured non-prompt ψ(2S) dimuon mass distribution in a typical p_T bin. The lines represent the result of the fit, which is simultaneously made to the eight mass distributions.

Since we have a much larger number of J/ψ events than ψ(2S) events, we need to use a slightly more complex J/ψ signal fit model. First, we noticed that the description of the peak line shape improves if we no longer impose that the two CB functions have a common mean; instead, we constrain μ_1 to be independent of p_T and leave μ_2 free in each p_T bin. Second, we add a Gaussian function, with μ_1 as mean and a normalization fixed from studies of the MC event samples, leading to a contribution of 3.5% of the total J/ψ yield. The Gaussian width, σ_G, is constrained to increase linearly with p_T with the same slope as σ_1 and σ_2. Simultaneously fitting all 19 J/ψ dimuon mass distributions provides a good description of the data. Fig. 2 (top) shows the non-prompt J/ψ dimuon mass distribution measured for one of the 19 p_T bins.

The most important shape parameters obtained from the dimuon mass fits (left free in each p_T bin) are the amplitude and slope of the continuum exponential function because they determine the fraction $f^{NPS}_{C_{NP}}$, which is computed by integrating the fitted background function (in each p_T bin) in the signal mass window (NPS) and dividing the result by the total number of events counted in that region. Fig. 3 shows the obtained $f^{NPS}_{C_{NP}}$ fractions, as functions of p_T.

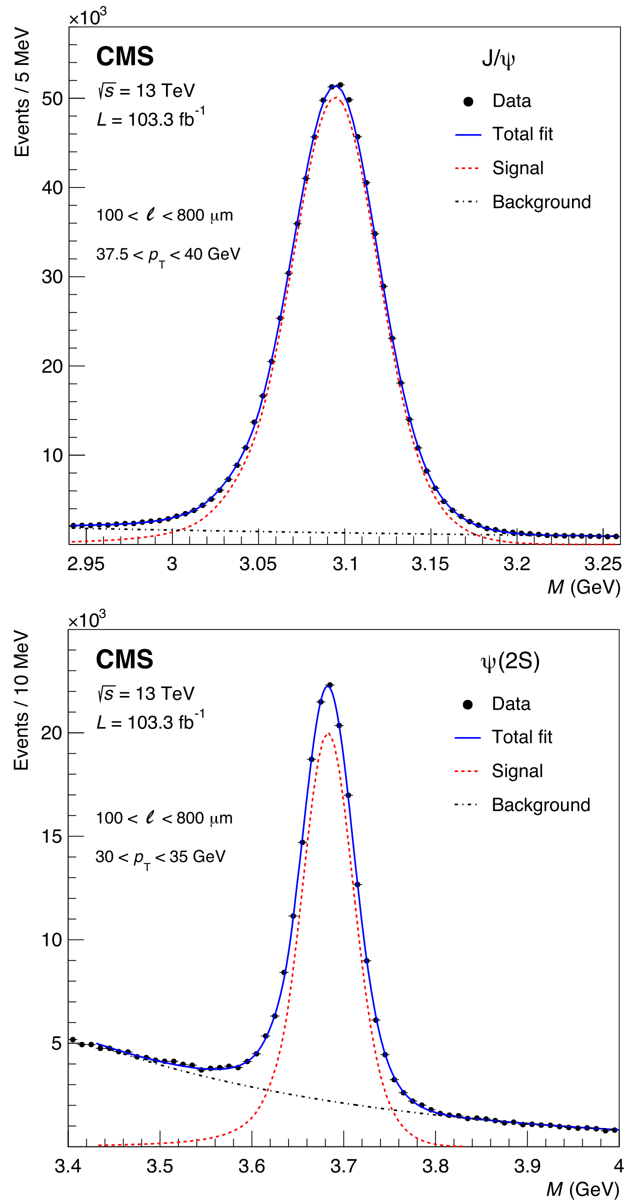

Fig. 2. Dimuon mass distributions measured for the non-prompt J/ψ (top) and ψ(2S) (bottom) event samples, in the mentioned p_T bins. The total fit function (blue), the sum of the two CB functions and, only in the J/ψ case, the Gaussian function (red), and the background continuum (black) are also shown.

3.3. Background fractions in the prompt charmonium signal regions

The fractions of continuum muon pairs in the prompt signal windows, $f^{PRS}_{C_{PR}}$, for both the J/ψ and ψ(2S) cases, are determined by fitting the dimuon mass distributions in the PR region ($|\ell| < 50\,\mu m$) using the same fit procedure and fit models as for the non-prompt cases; the only exception is that, now also in the J/ψ case, the two CB functions have the same μ parameter. Fig. 4 shows the dimuon mass distributions measured for the PR J/ψ and ψ(2S) events, in representative p_T bins, while Fig. 5 shows the p_T dependence of the background fraction $f^{PRS}_{C_{PR}}$.

The other source of background contributing to the PRS region corresponds to charmonia produced in decays of short-lived b hadrons. The fractions of events in the PRS windows due to those non-prompt charmonia, $f^{PRS}_{\psi_B}$, are obtained by fitting the decay length distributions of the dimuons in the J/ψ or ψ(2S) signal mass windows, while taking into consideration the existence of non-prompt continuum muon pairs. We

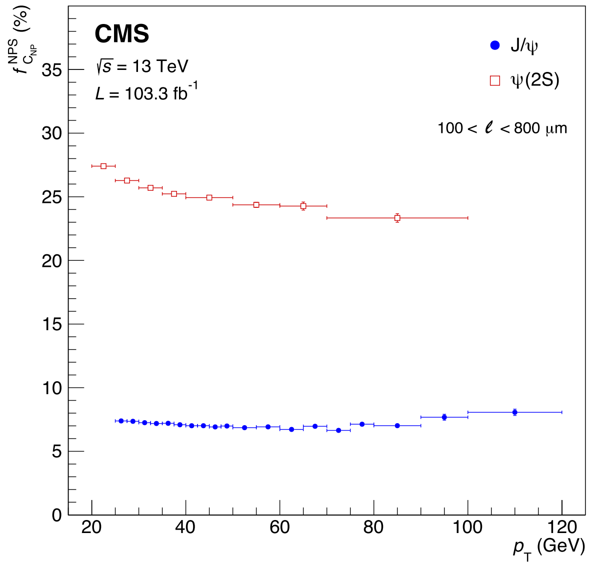

Fig. 3. Fraction of events in the NPS region due to continuum muon pairs, versus p_T, for the non-prompt J/ψ and ψ(2S) events.

simultaneously fit the 19 J/ψ or 8 ψ(2S) dimuon decay length distributions (one per p_T bin), in the range from −50 to +500 μm, selecting the events with dimuon mass in the mass signal windows. The fit model is composed of three contributions. First we have the prompt term, which is represented by the decay length resolution function, parameterized by the sum of three Gaussian functions with a common mean and independent widths, defined such that $\sigma_{G3} > \sigma_{G2} > \sigma_{G1}$. Studies of MC event samples show that the superposition of three Gaussian functions provides a good description of the prompt decay length distributions. They also show that the relative contributions of the three terms, their mean value μ, as well as the ratios σ_{G2}/σ_{G1} and σ_{G3}/σ_{G1}, are independent of p_T. Therefore, we impose such constraints in the fit model, so that the p_T-dependence of the decay length resolution is fully described by the σ_{G1} parameter, which is seen to decrease as p_T increases. The second term represents the contribution of ψ mesons from B decays and is parameterized by a decreasing exponential (for $\ell > 0$) convolved with the resolution function. The slope of this exponential function is left free in each p_T bin.

The third term represents the non-prompt continuum muon pairs, parameterized by one (for the J/ψ) or two (for the ψ(2S)) decreasing exponential functions convolved with the resolution function. This term is fixed, both in shape and normalization, by interpolating to the signal mass window the decay length distributions (in the 100–500 μm range) measured in the mass sidebands. The two J/ψ mass sidebands have identical decay length distributions, as seen in Fig. 6 (top), making the interpolation to the signal window a straightforward operation. In the case of the ψ(2S) analysis, the decay length distributions of the sideband events vary with dimuon mass. As shown in Fig. 6 (bottom), the highly populated and wide mass sidebands allow us to study the variations of the decay length distribution with mass using four mass bins in each of the two ψ(2S) sidebands. After finding that the shapes of the mass-sideband ψ(2S) decay length distributions do not show any p_T dependence, we imposed that the functional form representing the decay length distribution of this background term is independent of p_T.

Fig. 7 shows the dimuon decay length distributions measured in representative p_T bins for both charmonia, in the signal mass regions. The $f^{PRS}_{\psi_B}$ fractions are evaluated (in each p_T bin) by integrating the fitted ψ_B term in the prompt window and dividing the result by the total number of events counted in that region. The obtained fractions are shown in Fig. 8, for the J/ψ and ψ(2S) cases.

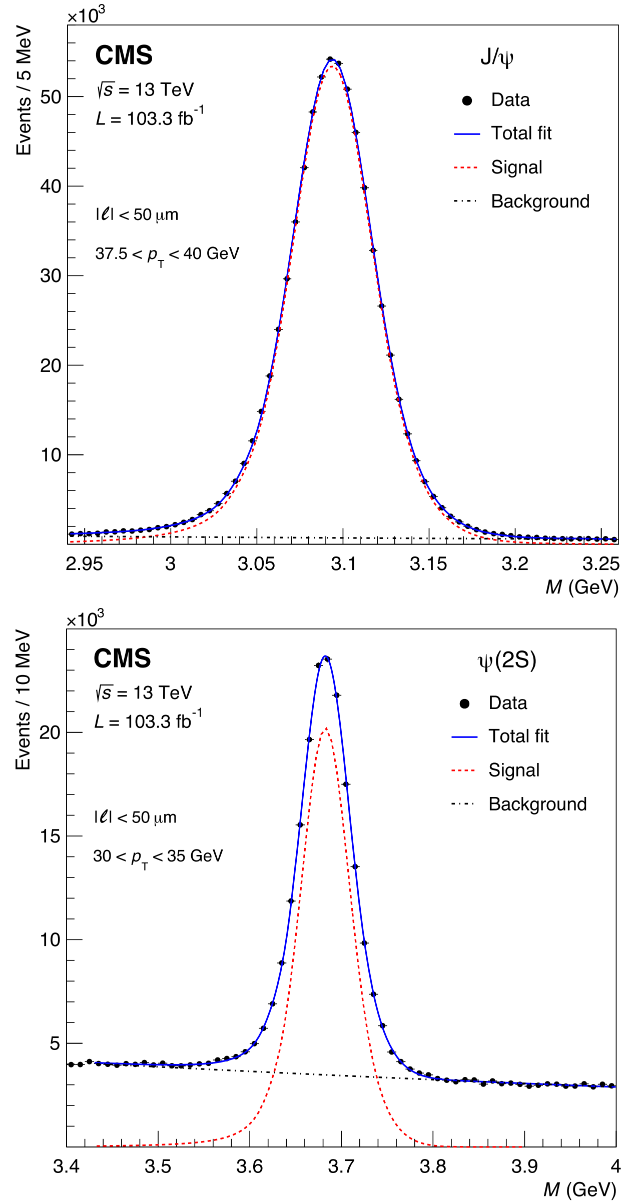

Fig. 4. Dimuon mass distributions measured for the prompt J/ψ (top) and ψ(2S) (bottom) event samples, in the mentioned p_T bins. The total fit function (blue), the sum of the two CB functions and (only in the J/ψ case) the Gaussian function (red), and the background continuum (black) are also shown.

4. Polarization measurement

For each p_T bin, the PRS and NPS $|\cos\vartheta_{HX}|$ distributions are directly obtained from the data, while the C_{PR} and C_{NP} distributions are evaluated as weighted averages of the continuum background events falling in the low and high mass sidebands, with weights determined by integrating the fitted dimuon mass background function in those sideband intervals (seen to be essentially independent of p_T and close to 50%, for both states). Fig. 9 shows the $|\cos\vartheta_{HX}|$ distributions measured in each of the two sidebands, plus their weighted average, for two representative p_T bins of the prompt J/ψ and non-prompt ψ(2S) samples.

The non-prompt J/ψ and ψ(2S) $|\cos\vartheta_{HX}|$ distributions are obtained, for each p_T bin, by subtracting from the NPS sample the non-prompt mass continuum background, as represented by Eq. (3), using the $|\cos\vartheta_{HX}|$ distributions interpolated from the mass sidebands scaled by the previously mentioned background fractions, $f_{C_{NP}}$. An analogous procedure is followed to measure the polarizations of the prompt J/ψ

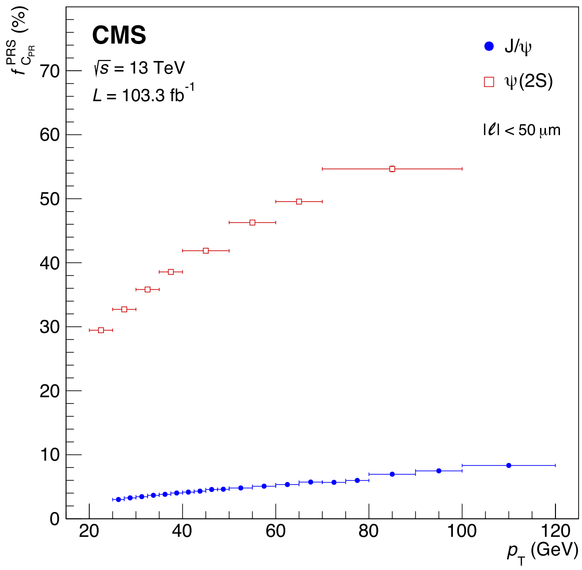

Fig. 5. Fraction of events in the PRS region due to continuum muon pairs, versus p_T, for the prompt J/ψ and ψ(2S) events.

and ψ(2S) mesons, the only difference being the extra subtraction of the charmonia produced in decays of B mesons that contaminate the PRS window, as represented by Eq. (4).

Fig. 10 (top) shows, for the J/ψ events and a representative p_T bin, the $|\cos\vartheta_{HX}|$ distributions of the PRS sample (in black), the ψ_B and C_{PR} contaminations (respectively in red and green, scaled by their fractions), and their difference, the prompt J/ψ signal (in blue). Fig. 10 (bottom) shows, for the ψ(2S) case and an illustrative p_T bin, the $|\cos\vartheta_{HX}|$ distributions of the NPS events (in black), of the interpolated continuum background events (in green, scaled by its fraction), and of their difference (in red), corresponding to the non-prompt ψ(2S) signal.

Fig. 11 shows the ratios between the measured and the simulated $|\cos\vartheta_{HX}|$ distributions, for the prompt and non-prompt J/ψ (top) and ψ(2S) (bottom) events, in the same p_T bins as used in the previous figures. Fitting these spectra with Eq. (2) gives the corresponding λ_ϑ values, for this specific p_T bin. As indicated by the curves, the fits do not include the $|\cos\vartheta_{HX}|$ bins closest to the edge of the covered range, corresponding to the ratio of two steeply falling distributions and where the uncertainties are more than twice those of the fitted $|\cos\vartheta_{HX}|$ bins. Repeating the same procedure for all p_T bins provides the p_T-dependence of the λ_ϑ parameters, for the prompt and non-prompt J/ψ and ψ(2S) states.

5. Systematic uncertainties

The analysis has been repeated with several variations in the procedure and input parameters, in order to evaluate the systematic uncertainties reflecting several potential effects.

The impact of possible differences between the 2017 and 2018 event samples has been evaluated by independently measuring the polarizations in each of the two samples. Since the results are compatible with each other, within their (independent) statistical uncertainties, no systematic uncertainty has been assigned.

The 5.6 GeV muon p_T threshold has been chosen to ensure that the selected muons have detection efficiencies in the plateau rather than in the low-p_T "turn-on region". In this way the analysis is robust with respect to small differences between the muon efficiencies in the measured and simulated event samples. Nevertheless, some residual effects could affect the muons in the $|\eta| < 0.3$ region. Such effects have been evaluated by redoing the analysis with several independent variations: rejecting events with at least one muon in the $0.2 < |\eta| < 0.3$ region, where the detection efficiency is lower because of the gap between

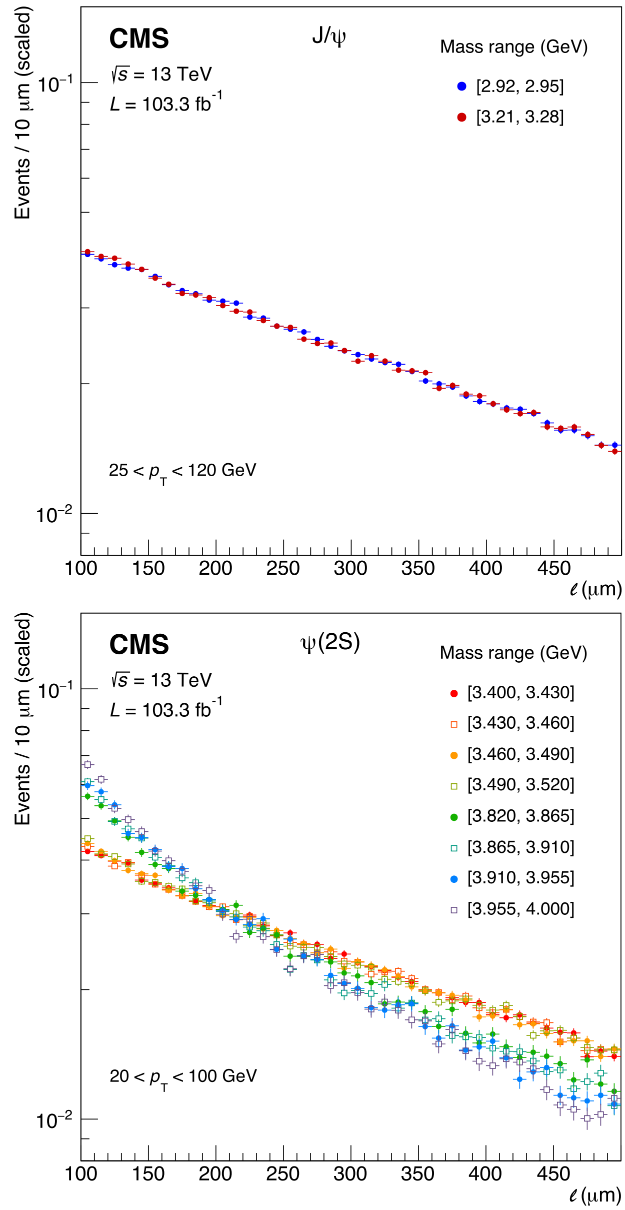

Fig. 6. Dimuon decay length distributions, integrated in p_T, measured for the sideband mass ranges mentioned in the legends, in the J/ψ (top) and ψ(2S) (bottom) cases.

the central muon detector wheel and its neighbors; increasing the p_T threshold value to 6.7 GeV for muons with $|\eta| < 0.2$, thereby completely avoiding the "turn-on region"; and applying very conservative variations to the p_T dependence of the simulated muon efficiency in the $|\eta| < 0.2$ region. Only the latter variation leads to a non-negligible variation (restricted to the lowest p_T region) with respect to the baseline analysis. We assign a (conservative) systematic uncertainty from this source, computed as the average of the absolute differences between the varied and baseline values, decreasing from ± 0.011 to zero as p_T increases from 25 to 50 GeV for the J/ψ analysis and from ± 0.014 to zero in the 20–40 GeV p_T range for the ψ(2S) case.

For $p_T \gtrsim 50$ GeV, the two daughter muons might be emitted with almost parallel trajectories and it can happen that, at the trigger level, they are detected as a single muon, in which case the event may not be selected [50,51]. While this effect is expected to be reproduced by the detailed trigger emulation included in the MC simulation, it is important to see if our results are sensitive to potential residual differences. By comparing the MC event distributions before and after applying the

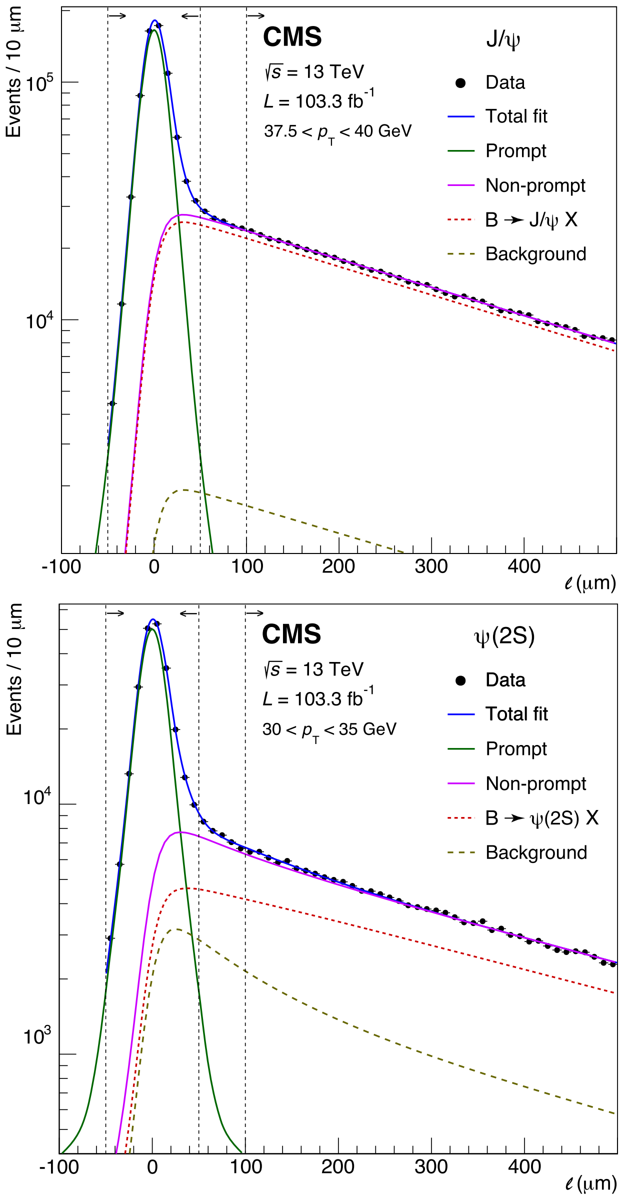

Fig. 7. Dimuon decay length distributions measured for the J/ψ (top) and ψ(2S) (bottom) cases, in their mass signal windows, in the mentioned p_T bins. The vertical dashed lines mark the limits of the PR and NP ranges. The total fit function, as well as the individual contributions, are also shown.

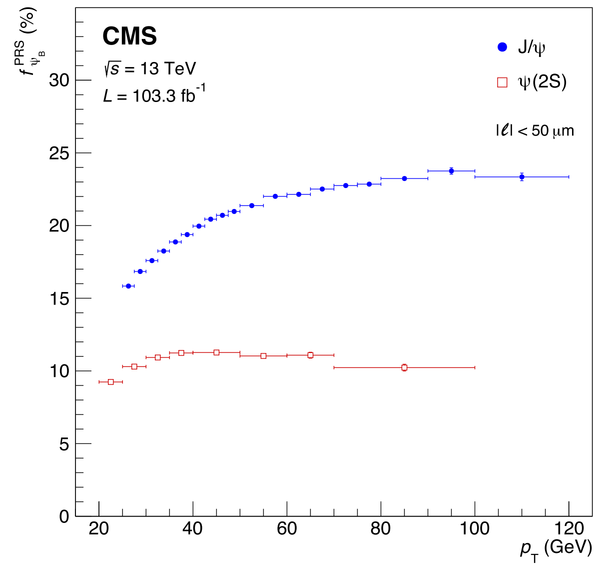

Fig. 8. Variation with p_T of the fraction of events in the PRS region from non-prompt J/ψ and ψ(2S) mesons.

dimuon trigger, we can evaluate the decrease in the dimuon trigger efficiency as the two muon trajectories approach each other in angular space (especially when they also have similar p_T values). Such MC studies allow us to define criteria that select events with low dimuon trigger efficiency [52], which we have rejected from the data analysis to evaluate the sensitivity of the measurement to a potentially inaccurate correction of this effect. We see no differences (beyond fluctuations caused by the reduction in the size of the event sample) between the baseline λ_ϑ values and those measured with the event sample obtained with the extra selection that rejects events with low dimuon detection efficiency. Therefore, we assign no systematic uncertainty to cover potential inaccuracies in the MC dimuon trigger emulation.

The J/ψ and ψ(2S) line shapes do not enter directly in the determination of the fractions of continuum muon pairs in the signal mass windows because we use, as denominator, the number of counted events. Furthermore, the signal fit model function is empirically chosen such that it describes well the simulated and measured peak shapes. Therefore, the dimuon mass signal shape should not have a significant impact on the evaluation of the continuum background fractions. This expectation has been confirmed through explicit tests, as those described in the following. In the case of the ψ(2S) analysis, the continuum dimuon background has a relatively high contribution, with respect to the ψ(2S) peak, so that it is important, for the polarization measurement, to precisely evaluate the fraction of events in the signal mass window coming from that background. The rather broad mass sideband ranges, both on the left and right sides of the ψ(2S) peak, allow us to evaluate the background fraction using an alternative procedure that completely avoids the necessity to describe the ψ(2S) peak: we simply count the number of events in each of the two signal-free sideband windows and then compute the interpolated event yield in the signal mass window, assuming that the mass distribution follows a decreasing exponential function. In other words, we only consider the mass ranges where the signal peak has a negligible contribution, if any, so that the background level can be computed without the need to describe the peak line shape. The counting method and the baseline fit procedure lead to indistinguishable results, confirming that the functional form used to describe the peak line shape does not bias the extraction of the background levels, so that we do not assign a systematic uncertainty to the ψ(2S) dimuon mass fit model.

In comparison with the ψ(2S) case, the low-mass sideband in the J/ψ analysis is relatively narrow and rather close to the left tail of the J/ψ peak, so that a small level of signal events could contaminate the sideband window, preventing the applicability of the counting method used in the ψ(2S) case. Instead, we have redone the fits of the dimuon mass distributions with variations of the J/ψ line shape tail, to evaluate if it could significantly contribute to the low-mass sideband window, thereby biasing the evaluation of the level of the continuum background. More specifically, we have redone the λ_ϑ measurement fixing the CB tail α parameter [49] to values equal to the baseline value plus or minus its fit uncertainty. The varied results are indistinguishable from the baseline measurement, so that we do not assign a systematic uncertainty reflecting the J/ψ dimuon mass fit model.

The fits of the decay length distributions include a term, corresponding to the non-prompt continuum dimuon background, that is fixed, in shape and normalization. While the shape is well parametrized by the selected functional form (a single exponential function for the J/ψ case and the sum of two exponential functions for the ψ(2S) case), the normalization is obtained with a certain statistical uncertainty. We have redone the prompt polarization measurement varying this normaliza-

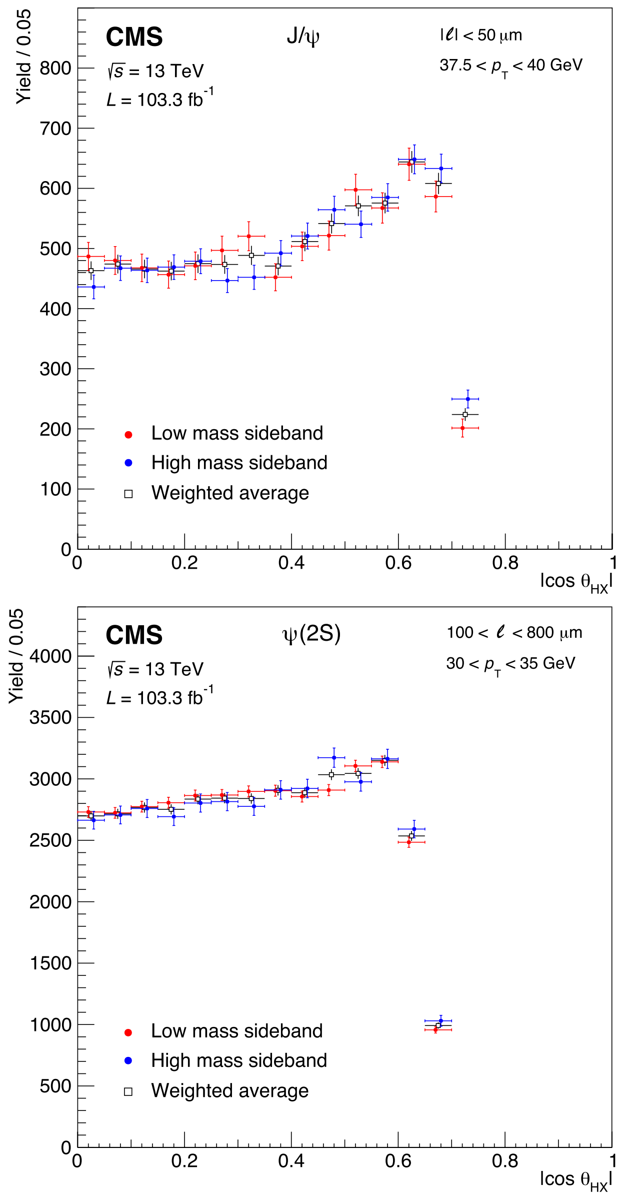

Fig. 9. $|\cos\vartheta_{HX}|$ distributions measured in the mass sidebands (shifted horizontally for better visibility), and their weighted average, for the prompt J/ψ (top) and non-prompt ψ(2S) (bottom) samples, in the mentioned p_T bins.

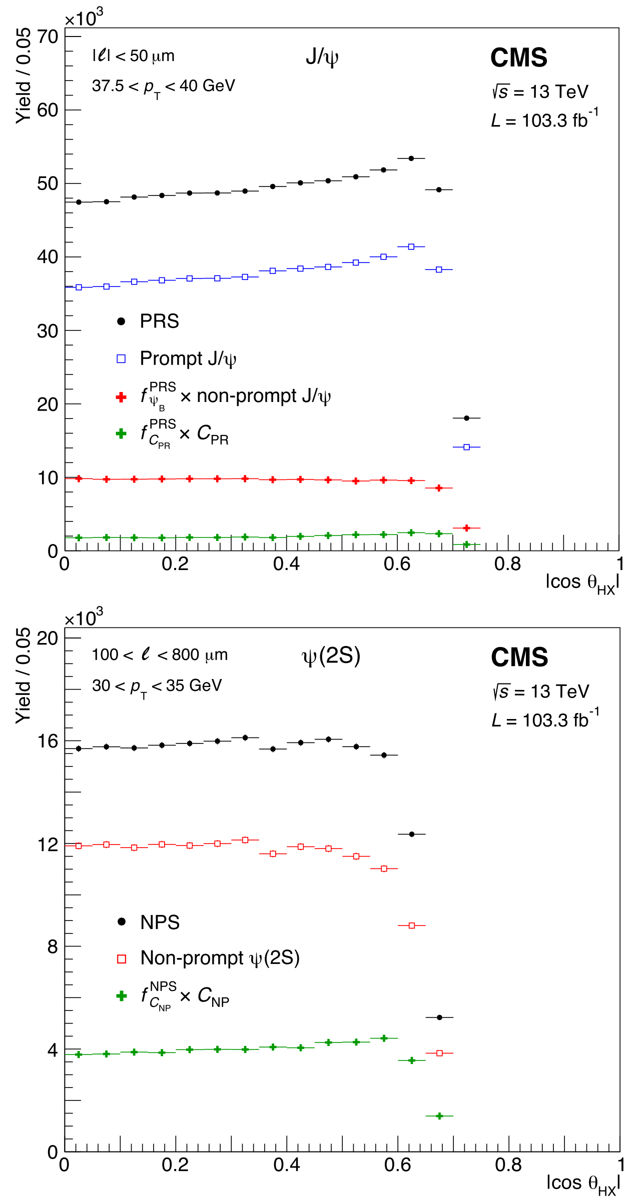

Fig. 10. $|\cos\vartheta_{HX}|$ distributions measured in the PRS J/ψ (top) and NPS ψ(2S) (bottom) samples, of the terms of Eqs. (4) and (3), respectively, in the mentioned p_T bins.

tion by adding or subtracting its uncertainty. The difference between the varied and baseline λ_ϑ values is compatible with zero, independently of p_T, so that no systematic uncertainty is assigned to this source.

In principle, measurements of quarkonium polarizations should be made by using Eq. (1) to fit the measured two-dimensional distributions of the polar and azimuthal decay angles [53]. The one-dimensional analysis we have done, integrating over the φ_{HX} angle and using Eq. (2), assumes that there are no correlations between $\cos\vartheta_{HX}$ and φ_{HX} in the two-dimensional acceptance maps. This assumption is expected to be valid in the helicity frame, for measurements made at mid-rapidity and sufficiently high p_T, as is the case of our analysis. To evaluate the uncertainty in the λ_ϑ results resulting from potential residual correlations, the analysis has been redone in exactly the same way but replacing $|\cos\vartheta_{HX}|$ by the φ_{HX} azimuthal angle and fitting the acceptance-corrected distributions with the function $1+\beta\cos 2\varphi_{HX}$, where $\beta = (2\,\lambda_\varphi)\,/\,(3+\lambda_\vartheta)$. As anticipated, the fitted values of β are almost zero, oscillating within the $|\beta| < 0.02$ range, for the prompt and non-prompt J/ψ and ψ(2S) mesons. It should be noted that small non-zero β values are not direct evidence of less-than-perfect MC simulations; even an ideal simulation can lead to acceptance-corrected distributions that exhibit small azimuthal anisotropies. The reason is that we are using the proton-proton HX frame and not the parton-parton HX frame, which would be the most suitable to measure the prompt polarizations. Similarly, measurements of non-prompt polarizations would ideally be made in the B meson rest frame, which is not known in our analysis. Since we must report the measurements in the proton-proton HX frame, small azimuthal anisotropies cannot be excluded, even if they are absent in the "natural frames". Nevertheless, to be conservative, we have considered that the residual non-flatness of the φ_{HX} distributions is caused by a mismatch between the simulated events and the measured ones. New $|\cos\vartheta_{HX}|$ vs. p_T acceptance maps have been obtained, reweighting each MC event by the weight $1+\beta\cos 2\varphi_{HX}$, using conservative β ranges compatible with the observed azimuthal anisotropies. Even though they are negligible with respect to the statistical uncertainty of the baseline results, we use the differences between the λ_ϑ values obtained with the alternative maps and those of the baseline analysis to assign a systematic uncertainty from

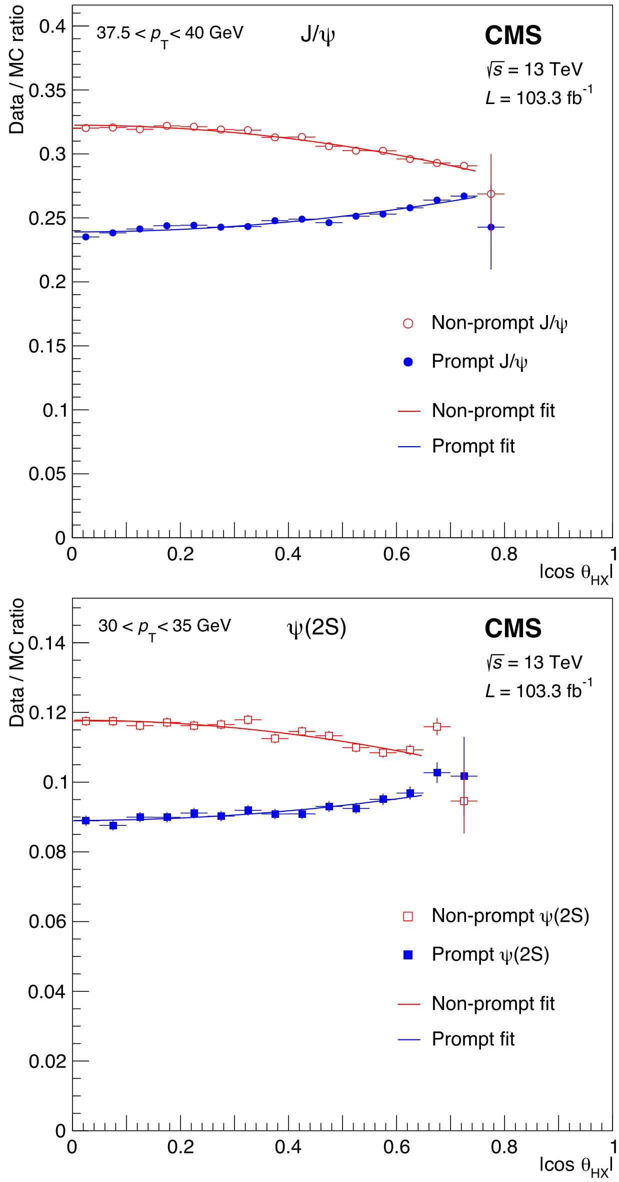

Fig. 11. Ratios between the measured and simulated $|\cos\vartheta_{HX}|$ distributions for the prompt and non-prompt J/ψ (top) and ψ(2S) (bottom) events, in the p_T bins mentioned in the legends. The curves represent fits using Eq. (2) and excluding the largest $|\cos\vartheta_{HX}|$ bins.

this source, varying from −0.004 (+0.005) to zero in the 25–37.5 GeV p_T range for the prompt (non-prompt) J/ψ polarizations and from −0.010 (+0.013) to zero in the 20–35 GeV p_T range for the prompt (non-prompt) ψ(2S) polarizations.

The systematic uncertainties, summed in quadrature, have a negligible contribution to the total uncertainties for $p_T \gtrsim 35$ GeV in the J/ψ results and for $p_T \gtrsim 30$ GeV in the ψ(2S) case.

6. Polarization results and discussion

Fig. 12 shows the λ_ϑ parameter measured for the non-prompt J/ψ and ψ(2S) mesons, as a function of p_T. For $p_T > 30$ GeV, the measured values show a flat p_T dependence, with λ_ϑ plateauing at around −0.2. No significant differences are seen between the J/ψ and ψ(2S) trends. The magenta and cyan bands represent the corresponding polarizations of J/ψ mesons produced in B → J/ψ X decays, computed in Ref. [54] and briefly described in the following. The J/ψ meson is intrinsically polarized along the direction of its emission in the B meson rest frame (the

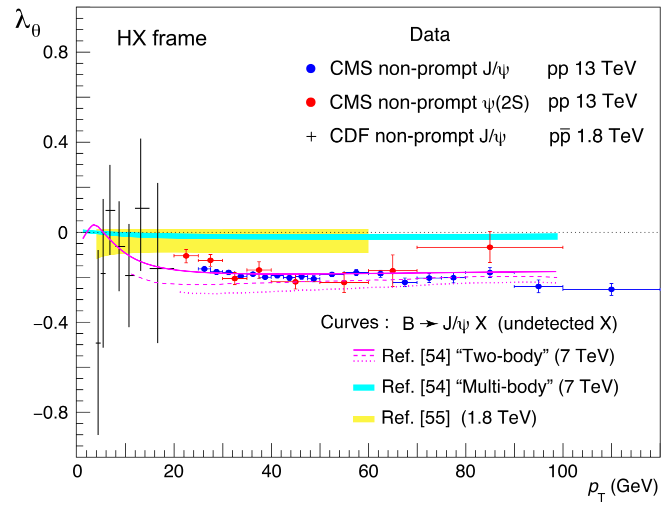

Fig. 12. The λ_ϑ parameter measured, as a function of p_T, for non-prompt J/ψ and ψ(2S) mesons. The vertical bars represent the total uncertainties. Predicted polarizations of J/ψ mesons produced in B → J/ψ X decays are shown for three calculations [54,55], discussed in the text. The low-p_T CDF measurement [56] is also shown.

cascade helicity axis, cHX), having, e.g., natural polarization $\lambda_0 = -1$ when X is a $J = 0$ particle. But in our "inclusive" non-prompt measurements we only observe the muons from the J/ψ decay, so that the dilepton distribution has to be referred to a direction (the HX axis) mostly uncorrelated from the natural cHX axis.

Since the J/ψ is emitted isotropically in the B meson rest frame, in the J/ψ rest frame the HX and cHX directions are distributed in a spherically uniform way with respect to one another, so that one could expect a fully smeared dilepton distribution ($\lambda_\vartheta = 0$) in the HX frame. However, that spherical symmetry is disrupted by the measurement process. For example, in each J/ψ p_T bin, the $\cos\Theta$ distribution, where Θ is the J/ψ emission angle in the B meson rest frame, defined with respect to the direction of the B meson in the laboratory, loses its natural uniformity and assumes a strongly modified shape, depending on the slope of the p_T distribution within the bin and on the mass of X [54]. The predictions shown in Fig. 12 correspond to two hypothetical cases. In the one concisely denoted by "two-body", X is a kaon or another $J = 0$ meson with similar or smaller mass: $\lambda_0 = -1$ and X has the kaon mass. The dashed and dotted curves reflect the requirement that the two J/ψ decay muons must have p_T values larger than 5 and 10 GeV, respectively, while the solid curve represents the calculation without any p_T requirement. The second, labeled as "multi-body", collectively considers all other systems of accompanying particles (including single particles of $J = 1$); the average λ_0 (of much smaller magnitude) and the X mass distribution were derived from J/ψ polarizations measured in the B rest frame by CLEO [57] and BaBar [58]. Comparing the data points and the computed curves indicates that non-prompt J/ψ production (at least for $p_T > 25$ GeV) is dominated by the "two-body" topology, where, interestingly, the J/ψ is expected to be predominantly produced through color-singlet processes [59,60].

The non-prompt J/ψ polarization measured by CDF [56] in p$\bar{\text{p}}$ collisions at $\sqrt{s} = 1.8$ TeV, in the $|y| < 0.6$ range, is also included, together with a computation, shown by the yellow band, made for the CDF conditions, where NRQCD color-octet contributions are found to dominate [55,61]. This prediction, leading to an almost vanishing non-prompt polarization, is in disagreement with our measurement.

Fig. 13 shows the λ_ϑ measurements obtained in this analysis for the prompt J/ψ (top) and ψ(2S) (bottom) mesons. The results previously reported by CMS and LHCb for pp collisions at $\sqrt{s} = 7$ TeV [10–12] are also shown, extending the p_T coverage down to much lower p_T. Considering all measurements together (neglecting possible variations with

Table 1
The λ_ϑ values measured in the HX frame, in bins of p_T, for the prompt and non-prompt J/ψ mesons, including the statistical (stat), systematic (syst), and total uncertainties.

p_T (GeV)	Prompt J/ψ				Non-prompt J/ψ			
	λ_ϑ	stat	syst	total	λ_ϑ	stat	syst	total
25–27.5	0.182	0.007	0.012	0.014	−0.163	0.006	0.011	0.013
27.5–30	0.193	0.008	0.009	0.012	−0.176	0.007	0.008	0.010
30–32.5	0.216	0.009	0.007	0.012	−0.178	0.007	0.007	0.010
32.5–35	0.208	0.010	0.006	0.012	−0.195	0.008	0.005	0.009
35–37.5	0.193	0.011	0.005	0.012	−0.186	0.009	0.005	0.010
37.5–40	0.204	0.013	0.004	0.013	−0.200	0.009	0.004	0.010
40–42.5	0.229	0.014	0.004	0.015	−0.193	0.010	0.003	0.011
42.5–45	0.223	0.016	0.003	0.017	−0.202	0.011	0.003	0.012
45–47.5	0.223	0.018	0.002	0.018	−0.197	0.012	0.002	0.012
47.5–50	0.221	0.021	0.001	0.021	−0.207	0.014	0.001	0.014
50–55	0.245	0.016	0.000	0.016	−0.188	0.010	0.000	0.010
55–60	0.266	0.021	0.000	0.021	−0.180	0.013	0.000	0.013
60–65	0.233	0.026	0.000	0.026	−0.184	0.016	0.000	0.016
65–70	0.271	0.034	0.000	0.034	−0.223	0.019	0.000	0.019
70–75	0.289	0.036	0.000	0.036	−0.204	0.019	0.000	0.019
75–80	0.216	0.041	0.000	0.041	−0.202	0.023	0.000	0.023
80–90	0.236	0.039	0.000	0.039	−0.179	0.021	0.000	0.021
90–100	0.357	0.059	0.000	0.059	−0.241	0.029	0.000	0.029
100–120	0.318	0.056	0.000	0.056	−0.254	0.026	0.000	0.026

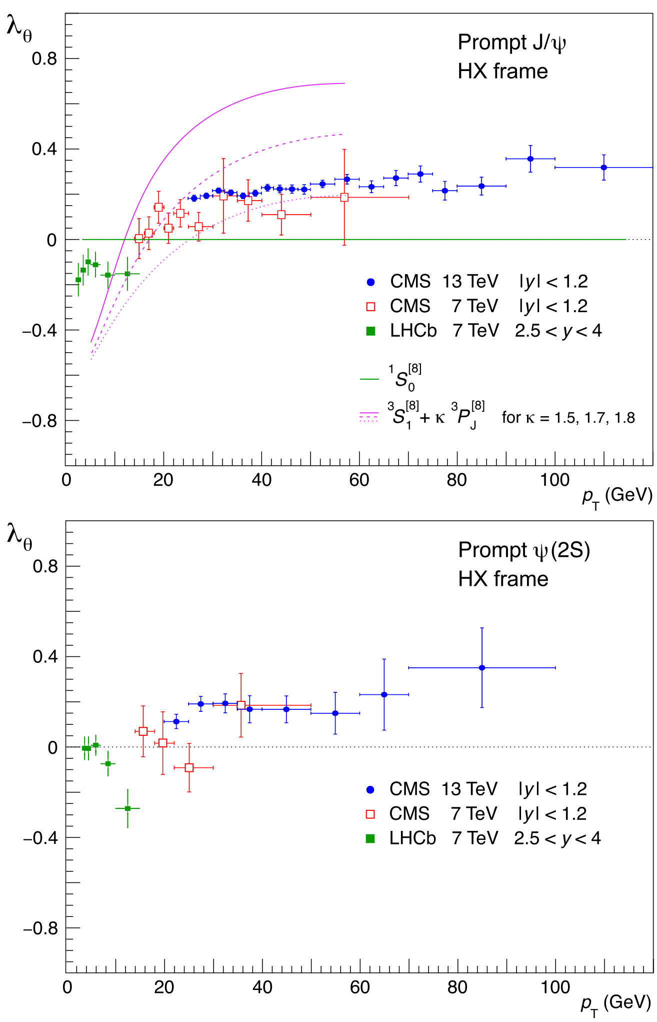

Fig. 13. The λ_ϑ parameter measured, as a function of p_T, for prompt J/ψ (top) and ψ(2S) (bottom) mesons, in pp collisions at $\sqrt{s} = 13$ TeV, compared to measurements made at 7 TeV by CMS [10] and LHCb [11,12]. The vertical bars represent the total uncertainties. The curves on the top panel are described in the text.

collision energy and rapidity interval), the λ_ϑ patterns show a significant trend from negative to positive, with the sign change occurring at $p_T \sim 15$ GeV. At high p_T, the polarizations tend to an asymptotic value, $\lambda_\vartheta \approx +0.3$. We see no evidence of the strong transverse polarizations (λ_ϑ approaching +1) expected in case the ${}^3S_1^{[8]}$ and ${}^3P_J^{[8]}$ octet terms would dominate.

It is interesting to compare the measured p_T dependence with the pattern obtainable as a superposition of the three dominant NRQCD color octet terms, ${}^1S_0^{[8]}$, ${}^3S_1^{[8]}$, and ${}^3P_J^{[8]}$. The first yields zero (p_T independent) polarization, while the remaining two, to be considered only in a mutual combination of the kind ${}^3S_1^{[8]} + \kappa\, {}^3P_J^{[8]}$ (the term ${}^3P_J^{[8]}$ is unphysical when considered alone, having $\lambda_\vartheta > +1$), are characterized by a λ_ϑ trend qualitatively similar to the measured one, going from longitudinal to transverse at a p_T transition point that depends on their relative proportions, symbolically represented by the κ coefficient. This behavior is illustrated by the family of curves displayed in Fig. 2 of Ref. [28], which are based on next-to-leading order calculations made for $\sqrt{s} = 7$ TeV and mid-rapidity [62,63]. Three examples of such polarized color-octet combinations are shown in Fig. 13 (top), in magenta, together with the unpolarized term, represented by the green horizontal line at zero. The comparison between the data points and the curves shows that precise polarization measurements significantly constrain the overall NRQCD color-octet contributions: the value of p_T where λ_ϑ changes sign determines κ, while the high-p_T asymptotic λ_ϑ value constrains the relative weight of the polarized (${}^3S_1^{[8]} + \kappa\, {}^3P_J^{[8]}$) and unpolarized (${}^1S_0^{[8]}$) color-octet terms.

The λ_ϑ values of the non-prompt and prompt J/ψ and ψ(2S) mesons reported in this Letter (corresponding to Figs. 12 and 13) are provided in Tables 1 and 2, as well as in the HEPData record for this analysis [64].

7. Summary

The prompt and non-prompt J/ψ and ψ(2S) λ_ϑ polarization parameters have been measured, in the helicity frame and for the $|y| < 1.2$ interval, using a sample of pp collisions at $\sqrt{s} = 13$ TeV collected in 2017 and 2018, corresponding to an integrated luminosity of 103.3 fb^{-1}. The results cover p_T ranges significantly broader than previous measurements: 25–120 and 20–100 GeV, for the J/ψ and ψ(2S), respectively.

The non-prompt J/ψ and ψ(2S) polarization measurements are compatible with each other, regarding the p_T dependence and the overall magnitude, plateauing at $\lambda_\vartheta \approx -0.2$ for $p_T > 30$ GeV. The measured

Table 2
The λ_ϑ values measured in the HX frame, as a function of p_T, for the prompt and non-prompt ψ(2S) mesons, indicating the statistical (stat), systematic (syst), and total uncertainties.

p_T (GeV)	Prompt ψ(2S)				Non-prompt ψ(2S)			
	λ_ϑ	stat	syst	total	λ_ϑ	stat	syst	total
20–25	0.112	0.028	0.018	0.033	−0.105	0.025	0.018	0.031
25–30	0.191	0.032	0.010	0.033	−0.125	0.024	0.010	0.026
30–35	0.193	0.041	0.006	0.042	−0.206	0.027	0.006	0.027
35–40	0.167	0.060	0.001	0.060	−0.168	0.036	0.001	0.036
40–50	0.167	0.059	0.000	0.059	−0.221	0.032	0.000	0.032
50–60	0.149	0.092	0.000	0.092	−0.223	0.043	0.000	0.043
60–70	0.232	0.157	0.000	0.157	−0.172	0.070	0.000	0.070
70–100	0.351	0.176	0.000	0.176	−0.067	0.069	0.000	0.069

trends agree with predictions based on the hypothesis that these charmonia are predominantly produced by two-body B meson decays, through color-singlet processes.

Regarding the prompt results, we see no evidence of strong transverse polarizations (λ_ϑ approaching +1), even at p_T values exceeding 30 times the J/ψ mass. Using NRQCD concepts, there is no evidence that, at very high p_T, the transversely polarized ${}^3S_1^{[8]}$ and ${}^3P_J^{[8]}$ octet terms become dominant with respect to the unpolarized ${}^1S_0^{[8]}$ octet. Taken together with previous CMS and LHCb measurements, covering a lower p_T domain, we see a significant variation of the prompt polarizations with p_T, at low p_T. These results will significantly constrain phenomenological analyses of charmonium production, so far mostly focused on p_T-differential cross sections.

Declaration of competing interest

The authors declare that they have no known competing financial interests or personal relationships that could have appeared to influence the work reported in this paper.

Data availability

Release and preservation of data used by the CMS Collaboration as the basis for publications is guided by the CMS data preservation, re-use and open access policy.

Acknowledgements

We congratulate our colleagues in the CERN accelerator departments for the excellent performance of the LHC and thank the technical and administrative staffs at CERN and at other CMS institutes for their contributions to the success of the CMS effort. In addition, we gratefully acknowledge the computing centers and personnel of the Worldwide LHC Computing Grid and other centers for delivering so effectively the computing infrastructure essential to our analyses. Finally, we acknowledge the enduring support for the construction and operation of the LHC, the CMS detector, and the supporting computing infrastructure provided by the following funding agencies: SC (Armenia), BMBWF and FWF (Austria); FNRS and FWO (Belgium); CNPq, CAPES, FAPERJ, FAPERGS, and FAPESP (Brazil); MES and BNSF (Bulgaria); CERN; CAS, MOST, and NSFC (China); Minciencias (Colombia); MSES and CSF (Croatia); RIF (Cyprus); SENESCYT (Ecuador); ERC PRG, RVTT3 and MoER TK202 (Estonia); Academy of Finland, MEC, and HIP (Finland); CEA and CNRS/IN2P3 (France); SRNSF (Georgia); BMBF, DFG, and HGF (Germany); GSRI (Greece); NKFIH (Hungary); DAE and DST (India); IPM (Iran); SFI (Ireland); INFN (Italy); MSIP and NRF (Republic of Korea); MES (Latvia); LMTLT (Lithuania); MOE and UM (Malaysia); BUAP, CINVESTAV, CONACYT, LNS, SEP, and UASLP-FAI (Mexico); MOS (Montenegro); MBIE (New Zealand); PAEC (Pakistan); MES and NSC (Poland); FCT (Portugal); MESTD (Serbia); MCIN/AEI and PCTI (Spain); MoSTR (Sri Lanka); Swiss Funding Agencies (Switzerland); MST (Taipei); MHESI and NSTDA (Thailand); TUBITAK and TENMAK (Turkey); NASU (Ukraine); STFC (United Kingdom); DOE and NSF (USA).

Individuals have received support from the Marie-Curie programme and the European Research Council and Horizon 2020 Grant, contract Nos. 675440, 724704, 752730, 758316, 765710, 824093, 101115353, 101002207, and COST Action CA16108 (European Union); the Leventis Foundation; the Alfred P. Sloan Foundation; the Alexander von Humboldt Foundation; the Science Committee, project no. 22rl-037 (Armenia); the Belgian Federal Science Policy Office; the Fonds pour la Formation à la Recherche dans l'Industrie et dans l'Agriculture (FRIA-Belgium); the Agentschap voor Innovatie door Wetenschap en Technologie (IWT-Belgium); the F.R.S.-FNRS and FWO (Belgium) under the "Excellence of Science – EOS" – be.h project n. 30820817; the Beijing Municipal Science & Technology Commission, No. Z191100007219010 and Fundamental Research Funds for the Central Universities (China); The Ministry of Education, Youth and Sports (MEYS) of the Czech Republic; the Shota Rustaveli National Science Foundation, grant FR-22-985 (Georgia); the Deutsche Forschungsgemeinschaft (DFG), under Germany's Excellence Strategy – EXC 2121 "Quantum Universe" – 390833306, and under project number 400140256 - GRK2497; the Hellenic Foundation for Research and Innovation (HFRI), Project Number 2288 (Greece); the Hungarian Academy of Sciences, the New National Excellence Program - ÚNKP, the NKFIH research grants K 131991, K 133046, K 138136, K 143460, K 143477, K 146913, K 146914, K 147048, 2020-2.2.1-ED-2021-00181, and TKP2021-NKTA-64 (Hungary); the Council of Science and Industrial Research, India; ICSC – National Research Centre for High Performance Computing, Big Data and Quantum Computing and FAIR – Future Artificial Intelligence Research, funded by the NextGenerationEU program (Italy); the Latvian Council of Science; the Ministry of Education and Science, project no. 2022/WK/14, and the National Science Center, contracts Opus 2021/41/B/ST2/01369 and 2021/43/B/ST2/01552 (Poland); the Fundação para a Ciência e a Tecnologia, grant CEECIND/01334/2018 (Portugal); the National Priorities Research Program by Qatar National Research Fund; MCIN/AEI/10.13039/501100011033, ERDF "a way of making Europe", and the Programa Estatal de Fomento de la Investigación Científica y Técnica de Excelencia María de Maeztu, grant MDM-2017-0765 and Programa Severo Ochoa del Principado de Asturias (Spain); the Chulalongkorn Academic into Its 2nd Century Project Advancement Project, and the National Science, Research and Innovation Fund via the Program Management Unit for Human Resources & Institutional Development, Research and Innovation, grant B37G660013 (Thailand); the Kavli Foundation; the Nvidia Corporation; the SuperMicro Corporation; the Welch Foundation, contract C-1845; and the Weston Havens Foundation (USA).

References

[1] N. Brambilla, et al., Quarkonium Working Group, Heavy quarkonium physics, CERN Yellow Reports: Monographs, CERN-2005-005, 2005, https://doi.org/10.

5170/CERN-2005-005, arXiv:hep-ph/0412158, published as CERN Yellow Report, CERN-2005-005.
[2] N. Brambilla, et al., Heavy quarkonium: progress, puzzles, and opportunities, Eur. Phys. J. C 71 (2011) 1534, https://doi.org/10.1140/epjc/s10052-010-1534-9, arXiv:1010.5827.
[3] G. Bodwin, E. Braaten, P. Lepage, Rigorous QCD analysis of inclusive annihilation and production of heavy quarkonium, Phys. Rev. D 51 (1995) 1125, https://doi.org/10.1103/PhysRevD.51.1125, arXiv:hep-ph/9407339, Erratum: https://doi.org/10.1103/PhysRevD.55.5853.
[4] R. Baier, R. Rückl, Hadronic production of J/ψ and Υ: transverse momentum distributions, Phys. Lett. B 102 (1981) 364, https://doi.org/10.1016/0370-2693(81)90636-5.
[5] J.-P. Lansberg, On the mechanisms of heavy-quarkonium hadroproduction, Eur. Phys. J. C 61 (2009) 693, https://doi.org/10.1140/epjc/s10052-008-0826-9, arXiv:0811.4005.
[6] V.D. Barger, W.-Y. Keung, R.J.N. Phillips, On ψ and Υ production via gluons, Phys. Lett. B 91 (1980) 253, https://doi.org/10.1016/0370-2693(80)90444-X.
[7] V.D. Barger, W.-Y. Keung, R.J.N. Phillips, Hadroproduction of ψ and Υ, Z. Phys. C 6 (1980) 169, https://doi.org/10.1007/BF01588844.
[8] F. Abe, et al., CDF, J/ψ and ψ(2S) production in $p\overline{p}$ collisions at $\sqrt{s} = 1.8$ TeV, Phys. Rev. Lett. 79 (1997) 572, https://doi.org/10.1103/PhysRevLett.79.572.
[9] T. Aaltonen, et al., CDF, Measurements of angular distributions of muons from Υ meson decays in $p\overline{p}$ collisions at $\sqrt{s} = 1.96$ TeV, Phys. Rev. Lett. 108 (2012) 151802, https://doi.org/10.1103/PhysRevLett.108.151802, arXiv:1112.1591.
[10] CMS Collaboration, Measurement of the prompt J/ψ and ψ(2S) polarizations in pp collisions at $\sqrt{s} = 7$ TeV, Phys. Lett. B 727 (2013) 381, https://doi.org/10.1016/j.physletb.2013.10.055, arXiv:1307.6070.
[11] LHCb Collaboration, Measurement of J/ψ polarization in pp collisions at $\sqrt{s} = 7$ TeV, Eur. Phys. J. C 73 (2013) 2631, https://doi.org/10.1140/epjc/s10052-013-2631-3, arXiv:1307.6379.
[12] LHCb Collaboration, Measurement of ψ(2S) polarisation in pp collisions at $\sqrt{s} = 7$ TeV, Eur. Phys. J. C 74 (2014) 2872, https://doi.org/10.1140/epjc/s10052-014-2872-9, arXiv:1403.1339.
[13] CMS Collaboration, Measurement of the Υ(1S), Υ(2S), and Υ(3S) polarizations in pp collisions at $\sqrt{s} = 7$ TeV, Phys. Rev. Lett. 110 (2013) 081802, https://doi.org/10.1103/PhysRevLett.110.081802, arXiv:1209.2922.
[14] LHCb Collaboration, Measurement of the Υ polarizations in pp collisions at $\sqrt{s} = 7$ and 8 TeV, J. High Energy Phys. 12 (2017) 110, https://doi.org/10.1007/JHEP12(2017)110, arXiv:1709.01301.
[15] M. Butenschön, B.A. Kniehl, J/ψ polarization at Tevatron and LHC: nonrelativistic-QCD factorization at the crossroads, Phys. Rev. Lett. 108 (2012) 172002, https://doi.org/10.1103/PhysRevLett.108.172002, arXiv:1201.1872.
[16] K.-T. Chao, Y.-Q. Ma, H.-S. Shao, K. Wang, Y.-J. Zhang, J/ψ polarization at hadron colliders in nonrelativistic QCD, Phys. Rev. Lett. 108 (2012) 242004, https://doi.org/10.1103/PhysRevLett.108.242004, arXiv:1201.2675.
[17] B. Gong, L.-P. Wan, J.-X. Wang, H.-F. Zhang, Polarization for prompt J/ψ and ψ(2S) production at the Tevatron and LHC, Phys. Rev. Lett. 110 (2013) 042002, https://doi.org/10.1103/PhysRevLett.110.042002, arXiv:1205.6682.
[18] M. Butenschön, B.A. Kniehl, Next-to-leading-order tests of NRQCD factorization with J/ψ yield and polarization, Mod. Phys. Lett. A 28 (2013) 1350027, https://doi.org/10.1142/S0217732313500272, arXiv:1212.2037.
[19] P. Faccioli, V. Knünz, C. Lourenço, J. Seixas, H. Wöhri, Quarkonium production in the LHC era: a polarized perspective, Phys. Lett. B 736 (2014) 98, https://doi.org/10.1016/j.physletb.2014.07.006, arXiv:1403.3970.
[20] G.T. Bodwin, K.-T. Chao, H.S. Chung, U.-R. Kim, J. Lee, Y.-Q. Ma, Fragmentation contributions to hadroproduction of prompt J/ψ, χ_{cJ}, and ψ(2S) states, Phys. Rev. D 93 (2016) 034041, https://doi.org/10.1103/PhysRevD.93.034041, arXiv:1509.07904.
[21] P. Faccioli, C. Lourenço, M. Araújo, J. Seixas, I. Krätschmer, V. Knünz, From identical S- and P-wave p_T spectra to maximally distinct polarizations: probing NRQCD with χ states, Eur. Phys. J. C 78 (2018) 268, https://doi.org/10.1140/epjc/s10052-018-5755-7, arXiv:1802.01106.
[22] V. Cheung, R. Vogt, Production and polarization of direct J/ψ to $O(\alpha_s^3)$ in the improved color evaporation model in collinear factorization, Phys. Rev. D 104 (2021) 094026, https://doi.org/10.1103/PhysRevD.104.094026, arXiv:2102.09118.
[23] A. Adare, et al., PHENIX, Transverse momentum dependence of J/ψ polarization at midrapidity in pp collisions at $s^{(1/2)} = 200$ GeV, Phys. Rev. D 82 (2010) 012001, https://doi.org/10.1103/PhysRevD.82.012001, arXiv:0912.2082.
[24] J. Adam, et al., STAR, Measurement of inclusive J/ψ polarization in pp collisions at $\sqrt{s} = 200$ GeV by the STAR experiment, Phys. Rev. D 102 (2020) 092009, https://doi.org/10.1103/PhysRevD.102.092009, arXiv:2007.04732.
[25] ALICE Collaboration, J/ψ polarization in pp collisions at $\sqrt{s} = 7$ TeV, Phys. Rev. Lett. 108 (2012) 082001, https://doi.org/10.1103/PhysRevLett.108.082001, arXiv:1111.1630.
[26] CMS Collaboration, Constraints on the χ_{c1} versus χ_{c2} polarizations in proton-proton collisions at $\sqrt{s} = 8$ TeV, Phys. Rev. Lett. 124 (2020) 162002, https://doi.org/10.1103/PhysRevLett.124.162002, arXiv:1912.07706.
[27] P. Faccioli, C. Lourenço, T. Madlener, From prompt to direct J/ψ production: new insights on the χ_{c1} and χ_{c2} polarizations and feed-down contributions from a global-fit analysis of mid-rapidity LHC data, Eur. Phys. J. C 80 (2020) 623, https://doi.org/10.1140/epjc/s10052-020-8201-6, arXiv:2006.15446.
[28] P. Faccioli, C. Lourenço, NRQCD colour-octet expansion vs. LHC quarkonium production: signs of a hierarchy puzzle?, Eur. Phys. J. C 79 (2019) 457, https://doi.org/10.1140/epjc/s10052-019-6968-0, arXiv:1905.09553.
[29] P. Faccioli, C. Lourenço, J. Seixas, H.K. Wöhri, Study of ψ(2S) and χ_c decays as feed-down sources of J/ψ hadro-production, J. High Energy Phys. 10 (2008) 004, https://doi.org/10.1088/1126-6708/2008/10/004, arXiv:0809.2153.
[30] P. Faccioli, C. Lourenço, J. Seixas, Rotation-invariant relations in vector meson decays into fermion pairs, Phys. Rev. Lett. 105 (2010) 061601, https://doi.org/10.1103/PhysRevLett.105.061601, arXiv:1005.2601.
[31] P. Faccioli, C. Lourenço, J. Seixas, New approach to quarkonium polarization studies, Phys. Rev. D 81 (2010) 111502(R), https://doi.org/10.1103/PhysRevD.81.111502, arXiv:1005.2855.
[32] P. Faccioli, C. Lourenço, Particle Polarization in High Energy Physics: an Introduction and Case Studies on Vector Particle Production at the LHC, Lecture Notes in Physics, Springer, 2022, https://doi.org/10.1007/978-3-031-08876-6.
[33] CMS Collaboration, Angular coefficients of Z bosons produced in pp collisions at $\sqrt{s} = 8$ TeV and decaying to $\mu^+\mu^-$ as a function of transverse momentum and rapidity, Phys. Lett. B 750 (2015) 154, https://doi.org/10.1016/j.physletb.2015.08.061, arXiv:1504.03512.
[34] ATLAS Collaboration, Measurement of the angular coefficients in Z-boson events using electron and muon pairs from data taken at $\sqrt{s} = 8$ TeV with the ATLAS detector, J. High Energy Phys. 08 (2016) 159, https://doi.org/10.1007/JHEP08(2016)159, arXiv:1606.00689.
[35] E. Braaten, D. Kang, J. Lee, C. Yu, Optimal spin quantization axes for the polarization of dileptons with large transverse momentum, Phys. Rev. D 79 (2009) 014025, https://doi.org/10.1103/PhysRevD.79.014025, arXiv:0810.4506.
[36] J.C. Collins, D.E. Soper, Angular distribution of dileptons in high-energy hadron collisions, Phys. Rev. D 16 (1977) 2219, https://doi.org/10.1103/PhysRevD.16.2219.
[37] CMS Collaboration, The CMS experiment at the CERN LHC, J. Instrum. 3 (2008) S08004, https://doi.org/10.1088/1748-0221/3/08/S08004.
[38] CMS Collaboration, Electron and photon reconstruction and identification with the CMS experiment at the CERN LHC, J. Instrum. 16 (2021) P05014, https://doi.org/10.1088/1748-0221/16/05/P05014, arXiv:2012.06888.
[39] CMS Collaboration, Performance of the CMS muon detector and muon reconstruction with proton-proton collisions at $\sqrt{s} = 13$ TeV, J. Instrum. 13 (2018) P06015, https://doi.org/10.1088/1748-0221/13/06/P06015, arXiv:1804.04528.
[40] CMS Collaboration, Description and performance of track and primary-vertex reconstruction with the CMS tracker, J. Instrum. 9 (2014) P10009, https://doi.org/10.1088/1748-0221/9/10/P10009, arXiv:1405.6569.
[41] CMS Collaboration, Performance of the CMS Level-1 trigger in proton-proton collisions at $\sqrt{s} = 13$ TeV, J. Instrum. 15 (2020) P10017, https://doi.org/10.1088/1748-0221/15/10/P10017, arXiv:2006.10165.
[42] CMS Collaboration, The CMS trigger system, J. Instrum. 12 (2017) P01020, https://doi.org/10.1088/1748-0221/12/01/P01020, arXiv:1609.02366.
[43] CMS Collaboration, CMS luminosity measurement for the 2017 data-taking period at $\sqrt{s} = 13$ TeV, CMS Physics Analysis Summary CMS-PAS-LUM-17-004, 2018, https://cds.cern.ch/record/2621960/.
[44] CMS Collaboration, CMS luminosity measurement for the 2018 data-taking period at $\sqrt{s} = 13$ TeV, CMS Physics Analysis Summary CMS-PAS-LUM-18-002, 2019, https://cds.cern.ch/record/2676164/.
[45] CMS Collaboration, Prompt and non-prompt J/ψ production in pp collisions at $\sqrt{s} = 7$ TeV, Eur. Phys. J. C 71 (2011) 1575, https://doi.org/10.1140/epjc/s10052-011-1575-8, arXiv:1011.4193.
[46] T. Sjöstrand, S. Ask, J.R. Christiansen, R. Corke, N. Desai, P. Ilten, S. Mrenna, S. Prestel, C.O. Rasmussen, P.Z. Skands, An introduction to PYTHIA 8.2, Comput. Phys. Commun. 191 (2015) 159, https://doi.org/10.1016/j.cpc.2015.01.024, arXiv:1410.3012.
[47] N. Davidson, T. Przedzinski, Z. Wąs, PHOTOS interface in C++: technical and physics documentation, Comput. Phys. Commun. 199 (2016) 86, https://doi.org/10.1016/j.cpc.2015.09.013, arXiv:1011.0937.
[48] S. Agostinelli, et al., GEANT4, GEANT4—a simulation toolkit, Nucl. Instrum. Methods Phys. Res., Sect. A 506 (2003) 250, https://doi.org/10.1016/S0168-9002(03)01368-8.
[49] M.J. Oreglia, A study of the reactions $\psi' \rightarrow \gamma\gamma\psi$, Ph.D. thesis, Stanford University, 1980, http://www.slac.stanford.edu/pubs/slacreports/slac-r-236.html.
[50] CMS Collaboration, J/ψ and ψ(2S) production in pp collisions at $\sqrt{s} = 7$ TeV, J. High Energy Phys. 02 (2012) 011, https://doi.org/10.1007/JHEP02(2012)011, arXiv:1111.1557.
[51] CMS Collaboration, Measurement of J/ψ and ψ(2S) prompt double-differential cross sections in pp collisions at $\sqrt{s} = 7$ TeV, Phys. Rev. Lett. 114 (2015) 191802, https://doi.org/10.1103/PhysRevLett.114.191802, arXiv:1502.04155.
[52] V. Knünz, Measurement of quarkonium polarization to probe QCD at the LHC, Ph.D. thesis, Tech. U., Atominst., Vienna, 2015, https://doi.org/10.1007/978-3-319-49935-2.
[53] P. Faccioli, C. Lourenço, J. Seixas, H. Wöhri, Towards the experimental clarification of quarkonium polarization, Eur. Phys. J. C 69 (2010) 657, https://doi.org/10.1140/epjc/s10052-010-1420-5, arXiv:1006.2738.
[54] P. Faccioli, C. Lourenço, On the polarization of the non-prompt contribution to inclusive J/ψ production in pp collisions, J. High Energy Phys. 10 (2022) 005, https://doi.org/10.1007/JHEP10(2022)010, arXiv:2206.14686.

[55] V. Krey, K.R.S. Balaji, Polarized J/ψ production from B mesons at the Fermilab Tevatron, Phys. Rev. D 67 (2003) 054011, https://doi.org/10.1103/PhysRevD.67.054011, arXiv:hep-ph/0209135.
[56] T. Affolder, et al., CDF, Measurement of J/ψ and ψ(2S) polarization in $p\overline{p}$ collisions at $\sqrt{s} = 1.8$ TeV, Phys. Rev. Lett. 85 (2000) 2886, https://doi.org/10.1103/PhysRevLett.85.2886, arXiv:hep-ex/0004027.
[57] R. Balest, et al., CLEO, Inclusive decays of B mesons to charmonium, Phys. Rev. D 52 (1995) 2661, https://doi.org/10.1103/PhysRevD.52.2661.
[58] B. Aubert, et al., BaBar, Study of inclusive production of charmonium mesons in B decay, Phys. Rev. D 67 (2003) 032002, https://doi.org/10.1103/PhysRevD.67.032002, arXiv:hep-ex/0207097.
[59] M. Beneke, F. Maltoni, I.Z. Rothstein, QCD analysis of inclusive B decay into charmonium, Phys. Rev. D 59 (1999) 054003, https://doi.org/10.1103/PhysRevD.59.054003, arXiv:hep-ph/9808360.
[60] M. Beneke, G.A. Schuler, S. Wolf, Quarkonium momentum distributions in photoproduction and B decay, Phys. Rev. D 62 (2000) 034004, https://doi.org/10.1103/PhysRevD.62.034004, arXiv:hep-ph/0001062.
[61] S. Fleming, O.F. Hernandez, I. Maksymyk, H. Nadeau, NRQCD matrix elements in polarization of J/ψ produced from b decay, Phys. Rev. D 55 (1997) 4098, https://doi.org/10.1103/PhysRevD.55.4098, arXiv:hep-ph/9608413.
[62] H.-S. Shao, Y.-Q. Ma, K. Wang, K.-T. Chao, Polarizations of χ_{c1} and χ_{c2} in prompt production at the LHC, Phys. Rev. Lett. 112 (2014) 182003, https://doi.org/10.1103/PhysRevLett.112.182003, arXiv:1402.2913.
[63] H.-S. Shao, HELAC-Onia 2.0: an upgraded matrix-element and event generator for heavy quarkonium physics, Comput. Phys. Commun. 198 (2016) 238, https://doi.org/10.1016/j.cpc.2015.09.011, arXiv:1507.03435.
[64] HEPData record for this analysis, https://doi.org/10.17182/hepdata.150034, 2024.

The CMS Collaboration

A. Hayrapetyan, A. Tumasyan [1]

Yerevan Physics Institute, Yerevan, Armenia

W. Adam, J.W. Andrejkovic, T. Bergauer, S. Chatterjee, K. Damanakis, M. Dragicevic, P.S. Hussain, M. Jeitler [2], N. Krammer, A. Li, D. Liko, I. Mikulec, J. Schieck [2], R. Schöfbeck, D. Schwarz, M. Sonawane, S. Templ, W. Waltenberger, C.-E. Wulz [2]

Institut für Hochenergiephysik, Vienna, Austria

M.R. Darwish [3], T. Janssen, T. Van Laer, P. Van Mechelen

Universiteit Antwerpen, Antwerpen, Belgium

N. Breugelmans, J. D'Hondt, S. Dansana, A. De Moor, M. Delcourt, F. Heyen, S. Lowette, I. Makarenko, D. Müller, S. Tavernier, M. Tytgat [4], G.P. Van Onsem, S. Van Putte, D. Vannerom

Vrije Universiteit Brussel, Brussel, Belgium

B. Bilin, B. Clerbaux, A.K. Das, G. De Lentdecker, H. Evard, L. Favart, P. Gianneios, J. Jaramillo, A. Khalilzadeh, F.A. Khan, K. Lee, M. Mahdavikhorrami, A. Malara, S. Paredes, M.A. Shahzad, L. Thomas, M. Vanden Bemden, C. Vander Velde, P. Vanlaer

Université Libre de Bruxelles, Bruxelles, Belgium

M. De Coen, D. Dobur, G. Gokbulut, Y. Hong, J. Knolle, L. Lambrecht, D. Marckx, K. Mota Amarilo, A. Samalan, K. Skovpen, N. Van Den Bossche, J. van der Linden, L. Wezenbeek

Ghent University, Ghent, Belgium

A. Benecke, A. Bethani, G. Bruno, C. Caputo, J. De Favereau De Jeneret, C. Delaere, I.S. Donertas, A. Giammanco, A.O. Guzel, Sa. Jain, V. Lemaitre, J. Lidrych, P. Mastrapasqua, T.T. Tran, S. Wertz

Université Catholique de Louvain, Louvain-la-Neuve, Belgium

G.A. Alves, M. Alves Gallo Pereira, E. Coelho, G. Correia Silva, C. Hensel, T. Menezes De Oliveira, C. Mora Herrera [5], A. Moraes, P. Rebello Teles, M. Soeiro, A. Vilela Pereira [5]

Centro Brasileiro de Pesquisas Fisicas, Rio de Janeiro, Brazil

W.L. Aldá Júnior, M. Barroso Ferreira Filho, H. Brandao Malbouisson, W. Carvalho, J. Chinellato [6], E.M. Da Costa, G.G. Da Silveira [7], D. De Jesus Damiao, S. Fonseca De Souza, R. Gomes De Souza,

M. Macedo, J. Martins[8], L. Mundim, H. Nogima, J.P. Pinheiro, A. Santoro, A. Sznajder, M. Thiel

Universidade do Estado do Rio de Janeiro, Rio de Janeiro, Brazil

C.A. Bernardes[7], L. Calligaris, T.R. Fernandez Perez Tomei, E.M. Gregores, B. Lopes Da Costa, I. Maietto Silverio, P.G. Mercadante, S.F. Novaes, B. Orzari, Sandra S. Padula

Universidade Estadual Paulista, Universidade Federal do ABC, São Paulo, Brazil

A. Aleksandrov, G. Antchev, R. Hadjiiska, P. Iaydjiev, M. Misheva, M. Shopova, G. Sultanov

Institute for Nuclear Research and Nuclear Energy, Bulgarian Academy of Sciences, Sofia, Bulgaria

A. Dimitrov, L. Litov, B. Pavlov, P. Petkov, A. Petrov, E. Shumka

University of Sofia, Sofia, Bulgaria

S. Keshri, S. Thakur

Instituto De Alta Investigación, Universidad de Tarapacá, Casilla 7 D, Arica, Chile

T. Cheng, T. Javaid, L. Yuan

Beihang University, Beijing, China

Z. Hu, Z. Liang, J. Liu, K. Yi[9,10]

Department of Physics, Tsinghua University, Beijing, China

G.M. Chen[11], H.S. Chen[11], M. Chen[11], F. Iemmi, C.H. Jiang, A. Kapoor[12], H. Liao, Z.-A. Liu[13], R. Sharma[14], J.N. Song[13], J. Tao, C. Wang[11], J. Wang, Z. Wang[11], H. Zhang, J. Zhao

Institute of High Energy Physics, Beijing, China

A. Agapitos, Y. Ban, S. Deng, B. Guo, C. Jiang, A. Levin, C. Li, Q. Li, Y. Mao, S. Qian, S.J. Qian, X. Qin, X. Sun, D. Wang, H. Yang, L. Zhang, Y. Zhao, C. Zhou

State Key Laboratory of Nuclear Physics and Technology, Peking University, Beijing, China

S. Yang

Guangdong Provincial Key Laboratory of Nuclear Science and Guangdong-Hong Kong Joint Laboratory of Quantum Matter, South China Normal University, Guangzhou, China

Z. You

Sun Yat-Sen University, Guangzhou, China

K. Jaffel, N. Lu

University of Science and Technology of China, Hefei, China

G. Bauer[15], B. Li, J. Zhang

Nanjing Normal University, Nanjing, China

X. Gao[16]

Institute of Modern Physics and Key Laboratory of Nuclear Physics and Ion-beam Application (MOE) - Fudan University, Shanghai, China

Z. Lin, C. Lu, M. Xiao

Zhejiang University, Hangzhou, Zhejiang, China

C. Avila, D.A. Barbosa Trujillo, A. Cabrera, C. Florez, J. Fraga, J.A. Reyes Vega

Universidad de Los Andes, Bogota, Colombia

F. Ramirez, C. Rendón, M. Rodriguez, A.A. Ruales Barbosa, J.D. Ruiz Alvarez

Universidad de Antioquia, Medellin, Colombia

D. Giljanovic, N. Godinovic, D. Lelas, A. Sculac

University of Split, Faculty of Electrical Engineering, Mechanical Engineering and Naval Architecture, Split, Croatia

M. Kovac, A. Petkovic, T. Sculac

University of Split, Faculty of Science, Split, Croatia

P. Bargassa, V. Brigljevic, B.K. Chitroda, D. Ferencek, K. Jakovcic, S. Mishra, A. Starodumov[17], T. Susa

Institute Rudjer Boskovic, Zagreb, Croatia

A. Attikis, K. Christoforou, A. Hadjiagapiou, C. Leonidou, J. Mousa, C. Nicolaou, L. Paizanos, F. Ptochos, P.A. Razis, H. Rykaczewski, H. Saka, A. Stepennov

University of Cyprus, Nicosia, Cyprus

M. Finger, M. Finger Jr., A. Kveton

Charles University, Prague, Czech Republic

E. Carrera Jarrin

Universidad San Francisco de Quito, Quito, Ecuador

Y. Assran[18,19], B. El-mahdy, S. Elgammal[19]

Academy of Scientific Research and Technology of the Arab Republic of Egypt, Egyptian Network of High Energy Physics, Cairo, Egypt

M.A. Mahmoud, Y. Mohammed

Center for High Energy Physics (CHEP-FU), Fayoum University, El-Fayoum, Egypt

K. Ehataht, M. Kadastik, T. Lange, S. Nandan, C. Nielsen, J. Pata, M. Raidal, L. Tani, C. Veelken

National Institute of Chemical Physics and Biophysics, Tallinn, Estonia

H. Kirschenmann, K. Osterberg, M. Voutilainen

Department of Physics, University of Helsinki, Helsinki, Finland

S. Bharthuar, N. Bin Norjoharuddeen, E. Brücken, F. Garcia, P. Inkaew, K.T.S. Kallonen, T. Lampén, K. Lassila-Perini, S. Lehti, T. Lindén, L. Martikainen, M. Myllymäki, M.m. Rantanen, H. Siikonen, J. Tuominiemi

Helsinki Institute of Physics, Helsinki, Finland

P. Luukka, H. Petrow

Lappeenranta-Lahti University of Technology, Lappeenranta, Finland

M. Besancon, F. Couderc, M. Dejardin, D. Denegri, J.L. Faure, F. Ferri, S. Ganjour, P. Gras, G. Hamel de Monchenault, M. Kumar, V. Lohezic, J. Malcles, F. Orlandi, L. Portales, A. Rosowsky, M.Ö. Sahin, A. Savoy-Navarro[20], P. Simkina, M. Titov, M. Tornago

IRFU, CEA, Université Paris-Saclay, Gif-sur-Yvette, France

F. Beaudette, G. Boldrini, P. Busson, A. Cappati, C. Charlot, M. Chiusi, F. Damas, O. Davignon, A. De Wit, I.T. Ehle, B.A. Fontana Santos Alves, S. Ghosh, A. Gilbert, R. Granier de Cassagnac, A. Hakimi, B. Harikrishnan, L. Kalipoliti, G. Liu, M. Nguyen, C. Ochando, R. Salerno, J.B. Sauvan, Y. Sirois, L. Urda Gómez, E. Vernazza, A. Zabi, A. Zghiche

Laboratoire Leprince-Ringuet, CNRS/IN2P3, Ecole Polytechnique, Institut Polytechnique de Paris, Palaiseau, France

J.-L. Agram[21], J. Andrea, D. Apparu, D. Bloch, J.-M. Brom, E.C. Chabert, C. Collard, S. Falke, U. Goerlach, R. Haeberle, A.-C. Le Bihan, M. Meena, O. Poncet, G. Saha, M.A. Sessini, P. Van Hove, P. Vaucelle

Université de Strasbourg, CNRS, IPHC UMR 7178, Strasbourg, France

A. Di Florio

Centre de Calcul de l'Institut National de Physique Nucleaire et de Physique des Particules, CNRS/IN2P3, Villeurbanne, France

D. Amram, S. Beauceron, B. Blancon, G. Boudoul, N. Chanon, D. Contardo, P. Depasse, C. Dozen[22], H. El Mamouni, J. Fay, S. Gascon, M. Gouzevitch, C. Greenberg, G. Grenier, B. Ille, E. Jourd'huy, I.B. Laktineh, M. Lethuillier, L. Mirabito, S. Perries, A. Purohit, M. Vander Donckt, P. Verdier, J. Xiao

Institut de Physique des 2 Infinis de Lyon (IP2I), Villeurbanne, France

A. Khvedelidze[17], I. Lomidze, Z. Tsamalaidze[17]

Georgian Technical University, Tbilisi, Georgia

V. Botta, S. Consuegra Rodríguez, L. Feld, K. Klein, M. Lipinski, D. Meuser, A. Pauls, D. Pérez Adán, N. Röwert, M. Teroerde

RWTH Aachen University, I. Physikalisches Institut, Aachen, Germany

S. Diekmann, A. Dodonova, N. Eich, D. Eliseev, F. Engelke, J. Erdmann, M. Erdmann, P. Fackeldey, B. Fischer, T. Hebbeker, K. Hoepfner, F. Ivone, A. Jung, M.y. Lee, F. Mausolf, M. Merschmeyer, A. Meyer, S. Mukherjee, D. Noll, F. Nowotny, A. Pozdnyakov, Y. Rath, W. Redjeb, F. Rehm, H. Reithler, V. Sarkisovi, A. Schmidt, A. Sharma, J.L. Spah, A. Stein, F. Torres Da Silva De Araujo[23], S. Wiedenbeck, S. Zaleski

RWTH Aachen University, III. Physikalisches Institut A, Aachen, Germany

C. Dziwok, G. Flügge, T. Kress, A. Nowack, O. Pooth, A. Stahl, T. Ziemons, A. Zotz

RWTH Aachen University, III. Physikalisches Institut B, Aachen, Germany

H. Aarup Petersen, M. Aldaya Martin, J. Alimena, S. Amoroso, Y. An, J. Bach, S. Baxter, M. Bayatmakou, H. Becerril Gonzalez, O. Behnke, A. Belvedere, S. Bhattacharya, F. Blekman[24], K. Borras[25], A. Campbell, A. Cardini, C. Cheng, F. Colombina, M. De Silva, G. Eckerlin, D. Eckstein, L.I. Estevez Banos, O. Filatov, E. Gallo[24], A. Geiser, V. Guglielmi, M. Guthoff, A. Hinzmann, L. Jeppe, B. Kaech, M. Kasemann, C. Kleinwort, R. Kogler, M. Komm, D. Krücker, W. Lange, D. Leyva Pernia, K. Lipka[26], W. Lohmann[27], F. Lorkowski, R. Mankel, I.-A. Melzer-Pellmann, M. Mendizabal Morentin, A.B. Meyer, G. Milella, K. Moral Figueroa, A. Mussgiller, L.P. Nair, J. Niedziela, A. Nürnberg, Y. Otarid, J. Park, E. Ranken, A. Raspereza, D. Rastorguev, J. Rübenach, L. Rygaard, A. Saggio, M. Scham[28,25], S. Schnake[25], P. Schütze, C. Schwanenberger[24], D. Selivanova, K. Sharko, M. Shchedrolosiev, D. Stafford, F. Vazzoler, A. Ventura Barroso, R. Walsh, D. Wang, Q. Wang, Y. Wen, K. Wichmann, L. Wiens[25], C. Wissing, Y. Yang, A. Zimermmane Castro Santos

Deutsches Elektronen-Synchrotron, Hamburg, Germany

A. Albrecht, S. Albrecht, M. Antonello, S. Bein, L. Benato, S. Bollweg, M. Bonanomi, P. Connor, K. El Morabit, Y. Fischer, E. Garutti, A. Grohsjean, J. Haller, H.R. Jabusch, G. Kasieczka, P. Keicher, R. Klanner, W. Korcari, T. Kramer, C.c. Kuo, V. Kutzner, F. Labe, J. Lange,

A. Lobanov, C. Matthies, L. Moureaux, M. Mrowietz, A. Nigamova, Y. Nissan, A. Paasch, K.J. Pena Rodriguez, T. Quadfasel, B. Raciti, M. Rieger, D. Savoiu, J. Schindler, P. Schleper, M. Schröder, J. Schwandt, M. Sommerhalder, H. Stadie, G. Steinbrück, A. Tews, M. Wolf

University of Hamburg, Hamburg, Germany

S. Brommer, M. Burkart, E. Butz, T. Chwalek, A. Dierlamm, A. Droll, N. Faltermann, M. Giffels, A. Gottmann, F. Hartmann[29], R. Hofsaess, M. Horzela, U. Husemann, J. Kieseler, M. Klute, R. Koppenhöfer, J.M. Lawhorn, M. Link, A. Lintuluoto, B. Maier, S. Maier, S. Mitra, M. Mormile, Th. Müller, M. Neukum, M. Oh, E. Pfeffer, M. Presilla, G. Quast, K. Rabbertz, B. Regnery, N. Shadskiy, I. Shvetsov, H.J. Simonis, L. Sowa, L. Stockmeier, K. Tauqeer, M. Toms, N. Trevisani, R.F. Von Cube, M. Wassmer, S. Wieland, F. Wittig, R. Wolf, X. Zuo

Karlsruher Institut fuer Technologie, Karlsruhe, Germany

G. Anagnostou, G. Daskalakis, A. Kyriakis, A. Papadopoulos[29], A. Stakia

Institute of Nuclear and Particle Physics (INPP), NCSR Demokritos, Aghia Paraskevi, Greece

P. Kontaxakis, G. Melachroinos, Z. Painesis, I. Papavergou, I. Paraskevas, N. Saoulidou, K. Theofilatos, E. Tziaferi, K. Vellidis, I. Zisopoulos

National and Kapodistrian University of Athens, Athens, Greece

G. Bakas, T. Chatzistavrou, G. Karapostoli, K. Kousouris, I. Papakrivopoulos, E. Siamarkou, G. Tsipolitis, A. Zacharopoulou

National Technical University of Athens, Athens, Greece

K. Adamidis, I. Bestintzanos, I. Evangelou, C. Foudas, C. Kamtsikis, P. Katsoulis, P. Kokkas, P.G. Kosmoglou Kioseoglou, N. Manthos, I. Papadopoulos, J. Strologas

University of Ioánnina, Ioánnina, Greece

C. Hajdu, D. Horvath[30,31], K. Márton, A.J. Rádl[32], F. Sikler, V. Veszpremi

HUN-REN Wigner Research Centre for Physics, Budapest, Hungary

M. Csanád, K. Farkas, A. Fehérkuti[33], M.M.A. Gadallah[34], Á. Kadlecsik, P. Major, G. Pásztor, G.I. Veres

MTA-ELTE Lendület CMS Particle and Nuclear Physics Group, Eötvös Loránd University, Budapest, Hungary

B. Ujvari, G. Zilizi

Faculty of Informatics, University of Debrecen, Debrecen, Hungary

G. Bencze, S. Czellar, J. Molnar, Z. Szillasi

Institute of Nuclear Research ATOMKI, Debrecen, Hungary

F. Nemes[33], T. Novak

Karoly Robert Campus, MATE Institute of Technology, Gyongyos, Hungary

J. Babbar, S. Bansal, S.B. Beri, V. Bhatnagar, G. Chaudhary, S. Chauhan, N. Dhingra[35], A. Kaur, A. Kaur, H. Kaur, M. Kaur, S. Kumar, K. Sandeep, T. Sheokand, J.B. Singh, A. Singla

Panjab University, Chandigarh, India

A. Ahmed, A. Bhardwaj, A. Chhetri, B.C. Choudhary, A. Kumar, A. Kumar, M. Naimuddin, K. Ranjan, M.K. Saini, S. Saumya

University of Delhi, Delhi, India

S. Baradia, S. Barman[36], S. Bhattacharya, S. Das Gupta, S. Dutta, S. Dutta, S. Sarkar

Saha Institute of Nuclear Physics, HBNI, Kolkata, India

M.M. Ameen, P.K. Behera, S.C. Behera, S. Chatterjee, G. Dash, P. Jana, P. Kalbhor, S. Kamble, J.R. Komaragiri[37], D. Kumar[37], P.R. Pujahari, N.R. Saha, A. Sharma, A.K. Sikdar, R.K. Singh, P. Verma, S. Verma, A. Vijay

Indian Institute of Technology Madras, Madras, India

S. Dugad, G.B. Mohanty, B. Parida, M. Shelake, P. Suryadevara

Tata Institute of Fundamental Research-A, Mumbai, India

A. Bala, S. Banerjee, R.M. Chatterjee, M. Guchait, Sh. Jain, A. Jaiswal, S. Kumar, G. Majumder, K. Mazumdar, S. Parolia, A. Thachayath

Tata Institute of Fundamental Research-B, Mumbai, India

S. Bahinipati[38], C. Kar, D. Maity[39], P. Mal, T. Mishra, V.K. Muraleedharan Nair Bindhu[39], K. Naskar[39], A. Nayak[39], S. Nayak, K. Pal, P. Sadangi, S.K. Swain, S. Varghese[39], D. Vats[39]

National Institute of Science Education and Research, An OCC of Homi Bhabha National Institute, Bhubaneswar, Odisha, India

S. Acharya[40], A. Alpana, S. Dube, B. Gomber[40], P. Hazarika, B. Kansal, A. Laha, B. Sahu[40], S. Sharma, K.Y. Vaish

Indian Institute of Science Education and Research (IISER), Pune, India

H. Bakhshiansohi[41], A. Jafari[42], M. Zeinali[43]

Isfahan University of Technology, Isfahan, Iran

S. Bashiri, S. Chenarani[44], S.M. Etesami, Y. Hosseini, M. Khakzad, E. Khazaie[45], M. Mohammadi Najafabadi, S. Tizchang[46]

Institute for Research in Fundamental Sciences (IPM), Tehran, Iran

M. Felcini, M. Grunewald

University College Dublin, Dublin, Ireland

M. Abbrescia[a,b], A. Colaleo[a,b], D. Creanza[a,c], B. D'Anzi[a,b], N. De Filippis[a,c], M. De Palma[a,b], W. Elmetenawee[a,b,47], L. Fiore[a], G. Iaselli[a,c], L. Longo[a], M. Louka[a,b], G. Maggi[a,c], M. Maggi[a], I. Margjeka[a], V. Mastrapasqua[a,b], S. My[a,b], S. Nuzzo[a,b], A. Pellecchia[a,b], A. Pompili[a,b], G. Pugliese[a,c], R. Radogna[a,b], D. Ramos[a], A. Ranieri[a], L. Silvestris[a], F.M. Simone[a,c], Ü. Sözbilir[a], A. Stamerra[a,b], D. Troiano[a,b], R. Venditti[a,b], P. Verwilligen[a], A. Zaza[a,b]

[a] *INFN Sezione di Bari, Bari, Italy*
[b] *Università di Bari, Bari, Italy*
[c] *Politecnico di Bari, Bari, Italy*

G. Abbiendi[a], C. Battilana[a,b], D. Bonacorsi[a,b], P. Capiluppi[a,b], A. Castro[a,b,†], F.R. Cavallo[a], M. Cuffiani[a,b], G.M. Dallavalle[a], T. Diotalevi[a,b], F. Fabbri[a], A. Fanfani[a,b], D. Fasanella[a], P. Giacomelli[a], L. Giommi[a,b], C. Grandi[a], L. Guiducci[a,b], S. Lo Meo[a,48], M. Lorusso[a,b], L. Lunerti[a], S. Marcellini[a], G. Masetti[a], F.L. Navarria[a,b], G. Paggi[a,b], A. Perrotta[a], F. Primavera[a,b], A.M. Rossi[a,b], S. Rossi Tisbeni[a,b], T. Rovelli[a,b], G.P. Siroli[a,b]

[a] *INFN Sezione di Bologna, Bologna, Italy*
[b] *Università di Bologna, Bologna, Italy*

S. Costa[a,b,49], A. Di Mattia[a], A. Lapertosa[a], R. Potenza[a,b], A. Tricomi[a,b,49], C. Tuve[a,b]

[a] *INFN Sezione di Catania, Catania, Italy*
[b] *Università di Catania, Catania, Italy*

P. Assiouras [a], G. Barbagli [a], G. Bardelli [a,b], B. Camaiani [a,b], A. Cassese [a], R. Ceccarelli [a], V. Ciulli [a,b], C. Civinini [a], R. D'Alessandro [a,b], E. Focardi [a,b], T. Kello [a], G. Latino [a,b], P. Lenzi [a,b], M. Lizzo [a], M. Meschini [a], S. Paoletti [a], A. Papanastassiou [a,b], G. Sguazzoni [a], L. Viliani [a]

[a] INFN Sezione di Firenze, Firenze, Italy
[b] Università di Firenze, Firenze, Italy

L. Benussi, S. Bianco, S. Meola [50], D. Piccolo

INFN Laboratori Nazionali di Frascati, Frascati, Italy

P. Chatagnon [a], F. Ferro [a], E. Robutti [a], S. Tosi [a,b]

[a] INFN Sezione di Genova, Genova, Italy
[b] Università di Genova, Genova, Italy

A. Benaglia [a], F. Brivio [a], F. Cetorelli [a,b], F. De Guio [a,b], M.E. Dinardo [a,b], P. Dini [a], S. Gennai [a], R. Gerosa [a,b], A. Ghezzi [a,b], P. Govoni [a,b], L. Guzzi [a], M.T. Lucchini [a,b], M. Malberti [a], S. Malvezzi [a], A. Massironi [a], D. Menasce [a], L. Moroni [a], M. Paganoni [a,b], S. Palluotto [a,b], D. Pedrini [a], A. Perego [a,b], B.S. Pinolini [a], G. Pizzati [a,b], S. Ragazzi [a,b], T. Tabarelli de Fatis [a,b]

[a] INFN Sezione di Milano-Bicocca, Milano, Italy
[b] Università di Milano-Bicocca, Milano, Italy

S. Buontempo [a], A. Cagnotta [a,b], F. Carnevali [a,b], N. Cavallo [a,c], F. Fabozzi [a,c], A.O.M. Iorio [a,b], L. Lista [a,b,51], P. Paolucci [a,29], B. Rossi [a]

[a] INFN Sezione di Napoli, Napoli, Italy
[b] Università di Napoli 'Federico II', Napoli, Italy
[c] Università della Basilicata, Potenza, Italy
[d] Scuola Superiore Meridionale (SSM), Napoli, Italy

R. Ardino [a], P. Azzi [a], N. Bacchetta [a,52], D. Bisello [a,b], P. Bortignon [a], G. Bortolato [a,b], A. Bragagnolo [a,b], A.C.M. Bulla [a], R. Carlin [a,b], P. Checchia [a], T. Dorigo [a], F. Gasparini [a,b], U. Gasparini [a,b], E. Lusiani [a], M. Margoni [a,b], A.T. Meneguzzo [a,b], M. Michelotto [a], M. Migliorini [a,b], J. Pazzini [a,b], P. Ronchese [a,b], R. Rossin [a,b], F. Simonetto [a,b], M. Tosi [a,b], A. Triossi [a,b], M. Zanetti [a,b], P. Zotto [a,b], A. Zucchetta [a,b], G. Zumerle [a,b]

[a] INFN Sezione di Padova, Padova, Italy
[b] Università di Padova, Padova, Italy
[c] Università di Trento, Trento, Italy

C. Aimè [a], A. Braghieri [a], S. Calzaferri [a], D. Fiorina [a], P. Montagna [a,b], V. Re [a], C. Riccardi [a,b], P. Salvini [a], I. Vai [a,b], P. Vitulo [a,b]

[a] INFN Sezione di Pavia, Pavia, Italy
[b] Università di Pavia, Pavia, Italy

S. Ajmal [a,b], M.E. Ascioti [a,b], G.M. Bilei [a], C. Carrivale [a,b], D. Ciangottini [a,b], L. Fanò [a,b], M. Magherini [a,b], V. Mariani [a,b], M. Menichelli [a], F. Moscatelli [a,53], A. Rossi [a,b], A. Santocchia [a,b], D. Spiga [a], T. Tedeschi [a,b]

[a] INFN Sezione di Perugia, Perugia, Italy
[b] Università di Perugia, Perugia, Italy

C.A. Alexe [a,c], P. Asenov [a,b], P. Azzurri [a], G. Bagliesi [a], R. Bhattacharya [a], L. Bianchini [a,b], T. Boccali [a], E. Bossini [a], D. Bruschini [a,c], R. Castaldi [a], M.A. Ciocci [a,b], M. Cipriani [a,b], V. D'Amante [a,d], R. Dell'Orso [a], S. Donato [a], A. Giassi [a], F. Ligabue [a,c], A.C. Marini [a], D. Matos Figueiredo [a], A. Messineo [a,b], M. Musich [a,b], F. Palla [a], A. Rizzi [a,b], G. Rolandi [a,c], S. Roy Chowdhury [a], T. Sarkar [a], A. Scribano [a], P. Spagnolo [a], R. Tenchini [a], G. Tonelli [a,b], N. Turini [a,d], F. Vaselli [a,c], A. Venturi [a], P.G. Verdini [a]

[a] INFN Sezione di Pisa, Pisa, Italy
[b] Università di Pisa, Pisa, Italy
[c] Scuola Normale Superiore di Pisa, Pisa, Italy
[d] Università di Siena, Siena, Italy

C. Baldenegro Barrera [a,b], P. Barria [a], C. Basile [a,b], M. Campana [a,b], F. Cavallari [a], L. Cunqueiro Mendez [a,b], D. Del Re [a,b], E. Di Marco [a,b], M. Diemoz [a], F. Errico [a,b], E. Longo [a,b], J. Mijuskovic [a,b], G. Organtini [a,b], F. Pandolfi [a], R. Paramatti [a,b], C. Quaranta [a,b], S. Rahatlou [a,b], C. Rovelli [a], F. Santanastasio [a,b], L. Soffi [a]

[a] INFN Sezione di Roma, Roma, Italy
[b] Sapienza Università di Roma, Roma, Italy

N. Amapane [a,b], R. Arcidiacono [a,c], S. Argiro [a,b], M. Arneodo [a,c], N. Bartosik [a], R. Bellan [a,b], A. Bellora [a,b], C. Biino [a], C. Borca [a,b], N. Cartiglia [a], M. Costa [a,b], R. Covarelli [a,b], N. Demaria [a], L. Finco [a], M. Grippo [a,b], B. Kiani [a,b], F. Legger [a], F. Luongo [a,b], C. Mariotti [a], L. Markovic [a,b], S. Maselli [a], A. Mecca [a,b], L. Menzio [a,b], P. Meridiani [a], E. Migliore [a,b], M. Monteno [a], R. Mulargia [a], M.M. Obertino [a,b], G. Ortona [a], L. Pacher [a,b], N. Pastrone [a], M. Pelliccioni [a], M. Ruspa [a,c], F. Siviero [a,b], V. Sola [a,b], A. Solano [a,b], A. Staiano [a], C. Tarricone [a,b], D. Trocino [a], G. Umoret [a,b], R. White [a,b]

[a] INFN Sezione di Torino, Torino, Italy
[b] Università di Torino, Torino, Italy
[c] Università del Piemonte Orientale, Novara, Italy

S. Belforte [a], V. Candelise [a,b], M. Casarsa [a], F. Cossutti [a], K. De Leo [a], G. Della Ricca [a,b]

[a] INFN Sezione di Trieste, Trieste, Italy
[b] Università di Trieste, Trieste, Italy

S. Dogra, J. Hong, C. Huh, B. Kim, J. Kim, D. Lee, H. Lee, S.W. Lee, C.S. Moon, Y.D. Oh, M.S. Ryu, S. Sekmen, B. Tae, Y.C. Yang

Kyungpook National University, Daegu, Korea

M.S. Kim

Department of Mathematics and Physics - GWNU, Gangneung, Korea

G. Bak, P. Gwak, H. Kim, D.H. Moon

Chonnam National University, Institute for Universe and Elementary Particles, Kwangju, Korea

E. Asilar, J. Choi, D. Kim, T.J. Kim, J.A. Merlin, Y. Ryou

Hanyang University, Seoul, Korea

S. Choi, S. Han, B. Hong, K. Lee, K.S. Lee, S. Lee, J. Yoo

Korea University, Seoul, Korea

J. Goh, S. Yang

Kyung Hee University, Department of Physics, Seoul, Korea

H.S. Kim, Y. Kim, S. Lee

Sejong University, Seoul, Korea

J. Almond, J.H. Bhyun, J. Choi, J. Choi, W. Jun, J. Kim, S. Ko, H. Kwon, H. Lee, J. Lee, J. Lee, B.H. Oh, S.B. Oh, H. Seo, U.K. Yang, I. Yoon

Seoul National University, Seoul, Korea

W. Jang, D.Y. Kang, Y. Kang, S. Kim, B. Ko, J.S.H. Lee, Y. Lee, I.C. Park, Y. Roh, I.J. Watson

University of Seoul, Seoul, Korea

S. Ha, H.D. Yoo

Yonsei University, Department of Physics, Seoul, Korea

M. Choi, M.R. Kim, H. Lee, Y. Lee, I. Yu

Sungkyunkwan University, Suwon, Korea

T. Beyrouthy, Y. Gharbia

College of Engineering and Technology, American University of the Middle East (AUM), Dasman, Kuwait

F. Alazemi

Kuwait University - College of Science - Department of Physics, Safat, Kuwait

K. Dreimanis, A. Gaile, G. Pikurs, A. Potrebko, M. Seidel, D. Sidiropoulos Kontos

Riga Technical University, Riga, Latvia

N.R. Strautnieks

University of Latvia (LU), Riga, Latvia

M. Ambrozas, A. Juodagalvis, A. Rinkevicius, G. Tamulaitis

Vilnius University, Vilnius, Lithuania

I. Yusuff[54], Z. Zolkapli

National Centre for Particle Physics, Universiti Malaya, Kuala Lumpur, Malaysia

J.F. Benitez, A. Castaneda Hernandez, H.A. Encinas Acosta, L.G. Gallegos Maríñez, M. León Coello, J.A. Murillo Quijada, A. Sehrawat, L. Valencia Palomo

Universidad de Sonora (UNISON), Hermosillo, Mexico

G. Ayala, H. Castilla-Valdez, H. Crotte Ledesma, E. De La Cruz-Burelo, I. Heredia-De La Cruz[55], R. Lopez-Fernandez, J. Mejia Guisao, C.A. Mondragon Herrera, A. Sánchez Hernández

Centro de Investigacion y de Estudios Avanzados del IPN, Mexico City, Mexico

C. Oropeza Barrera, D.L. Ramirez Guadarrama, M. Ramírez García

Universidad Iberoamericana, Mexico City, Mexico

I. Bautista, I. Pedraza, H.A. Salazar Ibarguen, C. Uribe Estrada

Benemerita Universidad Autonoma de Puebla, Puebla, Mexico

I. Bubanja, N. Raicevic

University of Montenegro, Podgorica, Montenegro

P.H. Butler

University of Canterbury, Christchurch, New Zealand

A. Ahmad, M.I. Asghar, A. Awais, M.I.M. Awan, H.R. Hoorani, W.A. Khan

National Centre for Physics, Quaid-I-Azam University, Islamabad, Pakistan

V. Avati, L. Grzanka, M. Malawski

AGH University of Krakow, Faculty of Computer Science, Electronics and Telecommunications, Krakow, Poland

H. Bialkowska, M. Bluj, M. Górski, M. Kazana, M. Szleper, P. Zalewski

National Centre for Nuclear Research, Swierk, Poland

K. Bunkowski, K. Doroba, A. Kalinowski, M. Konecki, J. Krolikowski, A. Muhammad

Institute of Experimental Physics, Faculty of Physics, University of Warsaw, Warsaw, Poland

K. Pozniak, W. Zabolotny

Warsaw University of Technology, Warsaw, Poland

M. Araujo, D. Bastos, C. Beirão Da Cruz E Silva, A. Boletti, M. Bozzo, T. Camporesi, G. Da Molin, P. Faccioli, M. Gallinaro, J. Hollar, N. Leonardo, G.B. Marozzo, T. Niknejad, A. Petrilli, M. Pisano, J. Seixas, J. Varela, J.W. Wulff

Laboratório de Instrumentação e Física Experimental de Partículas, Lisboa, Portugal

P. Adzic, P. Milenovic

Faculty of Physics, University of Belgrade, Belgrade, Serbia

M. Dordevic, J. Milosevic, V. Rekovic

VINCA Institute of Nuclear Sciences, University of Belgrade, Belgrade, Serbia

J. Alcaraz Maestre, Cristina F. Bedoya, Oliver M. Carretero, M. Cepeda, M. Cerrada, N. Colino, B. De La Cruz, A. Delgado Peris, A. Escalante Del Valle, D. Fernández Del Val, J.P. Fernández Ramos, J. Flix, M.C. Fouz, O. Gonzalez Lopez, S. Goy Lopez, J.M. Hernandez, M.I. Josa, E. Martin Viscasillas, D. Moran, C.M. Morcillo Perez, Á. Navarro Tobar, C. Perez Dengra, A. Pérez-Calero Yzquierdo, J. Puerta Pelayo, I. Redondo, S. Sánchez Navas, J. Sastre, J. Vazquez Escobar

Centro de Investigaciones Energéticas Medioambientales y Tecnológicas (CIEMAT), Madrid, Spain

J.F. de Trocóniz

Universidad Autónoma de Madrid, Madrid, Spain

B. Alvarez Gonzalez, J. Cuevas, J. Fernandez Menendez, S. Folgueras, I. Gonzalez Caballero, J.R. González Fernández, P. Leguina, E. Palencia Cortezon, J. Prado Pico, C. Ramón Álvarez, V. Rodríguez Bouza, A. Soto Rodríguez, A. Trapote, C. Vico Villalba, P. Vischia

Universidad de Oviedo, Instituto Universitario de Ciencias y Tecnologías Espaciales de Asturias (ICTEA), Oviedo, Spain

S. Bhowmik, S. Blanco Fernández, J.A. Brochero Cifuentes, I.J. Cabrillo, A. Calderon, J. Duarte Campderros, M. Fernandez, G. Gomez, C. Lasaosa García, R. Lopez Ruiz, C. Martinez Rivero, P. Martinez Ruiz del Arbol, F. Matorras, P. Matorras Cuevas, E. Navarrete Ramos, J. Piedra Gomez, L. Scodellaro, I. Vila, J.M. Vizan Garcia

Instituto de Física de Cantabria (IFCA), CSIC-Universidad de Cantabria, Santander, Spain

B. Kailasapathy[56], D.D.C. Wickramarathna

University of Colombo, Colombo, Sri Lanka

W.G.D. Dharmaratna[57], K. Liyanage, N. Perera

University of Ruhuna, Department of Physics, Matara, Sri Lanka

D. Abbaneo, C. Amendola, E. Auffray, G. Auzinger, J. Baechler, D. Barney, A. Bermúdez Martínez, M. Bianco, A.A. Bin Anuar, A. Bocci, L. Borgonovi, C. Botta, E. Brondolin, C. Caillol, G. Cerminara, N. Chernyavskaya, D. d'Enterria, A. Dabrowski, A. David, A. De Roeck, M.M. Defranchis, M. Deile, M. Dobson, G. Franzoni, W. Funk, S. Giani, D. Gigi, K. Gill, F. Glege, J. Hegeman, J.K. Heikkilä, B. Huber, V. Innocente, T. James, P. Janot, O. Kaluzinska, O. Karacheban[27], S. Laurila, P. Lecoq, E. Leutgeb, C. Lourenço, L. Malgeri, M. Mannelli, M. Matthewman, A. Mehta, F. Meijers, S. Mersi, E. Meschi, V. Milosevic, F. Monti, F. Moortgat, M. Mulders, I. Neutelings, S. Orfanelli, F. Pantaleo,

G. Petrucciani, A. Pfeiffer, M. Pierini, H. Qu, D. Rabady, B. Ribeiro Lopes, M. Rovere, H. Sakulin, S. Sanchez Cruz, S. Scarfi, C. Schwick, M. Selvaggi, A. Sharma, K. Shchelina, P. Silva, P. Sphicas [58], A.G. Stahl Leiton, A. Steen, S. Summers, D. Treille, P. Tropea, D. Walter, J. Wanczyk [59], J. Wang, S. Wuchterl, P. Zehetner, P. Zejdl, W.D. Zeuner

CERN, European Organization for Nuclear Research, Geneva, Switzerland

T. Bevilacqua [60], L. Caminada [60], A. Ebrahimi, W. Erdmann, R. Horisberger, Q. Ingram, H.C. Kaestli, D. Kotlinski, C. Lange, M. Missiroli [60], L. Noehte [60], T. Rohe

Paul Scherrer Institut, Villigen, Switzerland

T.K. Aarrestad, K. Androsov [59], M. Backhaus, G. Bonomelli, A. Calandri, C. Cazzaniga, K. Datta, P. De Bryas Dexmiers D'archiac [59], A. De Cosa, G. Dissertori, M. Dittmar, M. Donegà, F. Eble, M. Galli, K. Gedia, F. Glessgen, C. Grab, N. Härringer, T.G. Harte, D. Hits, W. Lustermann, A.-M. Lyon, R.A. Manzoni, M. Marchegiani, L. Marchese, C. Martin Perez, A. Mascellani [59], F. Nessi-Tedaldi, F. Pauss, V. Perovic, S. Pigazzini, C. Reissel, T. Reitenspiess, B. Ristic, F. Riti, R. Seidita, J. Steggemann [59], A. Tarabini, D. Valsecchi, R. Wallny

ETH Zurich - Institute for Particle Physics and Astrophysics (IPA), Zurich, Switzerland

C. Amsler [61], P. Bärtschi, M.F. Canelli, K. Cormier, M. Huwiler, W. Jin, A. Jofrehei, B. Kilminster, S. Leontsinis, S.P. Liechti, A. Macchiolo, P. Meiring, F. Meng, U. Molinatti, J. Motta, A. Reimers, P. Robmann, M. Senger, E. Shokr, F. Stäger, R. Tramontano

Universität Zürich, Zurich, Switzerland

C. Adloff [62], D. Bhowmik, C.M. Kuo, W. Lin, P.K. Rout, P.C. Tiwari [37], S.S. Yu

National Central University, Chung-Li, Taiwan

L. Ceard, K.F. Chen, P.s. Chen, Z.g. Chen, A. De Iorio, W.-S. Hou, T.h. Hsu, Y.w. Kao, S. Karmakar, G. Kole, Y.y. Li, R.-S. Lu, E. Paganis, X.f. Su, J. Thomas-Wilsker, L.s. Tsai, H.y. Wu, E. Yazgan

National Taiwan University (NTU), Taipei, Taiwan

C. Asawatangtrakuldee, N. Srimanobhas, V. Wachirapusitanand

High Energy Physics Research Unit, Department of Physics, Faculty of Science, Chulalongkorn University, Bangkok, Thailand

D. Agyel, F. Boran, F. Dolek, I. Dumanoglu [63], E. Eskut, Y. Guler [64], E. Gurpinar Guler [64], C. Isik, O. Kara, A. Kayis Topaksu, U. Kiminsu, G. Onengut, K. Ozdemir [65], A. Polatoz, B. Tali [66], U.G. Tok, S. Turkcapar, E. Uslan, I.S. Zorbakir

Çukurova University, Physics Department, Science and Art Faculty, Adana, Turkey

G. Sokmen, M. Yalvac [67]

Middle East Technical University, Physics Department, Ankara, Turkey

B. Akgun, I.O. Atakisi, E. Gülmez, M. Kaya [68], O. Kaya [69], S. Tekten [70]

Bogazici University, Istanbul, Turkey

A. Cakir, K. Cankocak [63,71], G.G. Dincer [63], Y. Komurcu, S. Sen [72]

Istanbul Technical University, Istanbul, Turkey

O. Aydilek [73], B. Hacisahinoglu, I. Hos [74], B. Kaynak, S. Ozkorucuklu, O. Potok, H. Sert, C. Simsek, C. Zorbilmez

Istanbul University, Istanbul, Turkey

S. Cerci [66], B. Isildak [75], D. Sunar Cerci, T. Yetkin

Yildiz Technical University, Istanbul, Turkey

A. Boyaryntsev, B. Grynyov

Institute for Scintillation Materials of National Academy of Science of Ukraine, Kharkiv, Ukraine

L. Levchuk

National Science Centre, Kharkiv Institute of Physics and Technology, Kharkiv, Ukraine

D. Anthony, J.J. Brooke, A. Bundock, F. Bury, E. Clement, D. Cussans, H. Flacher, M. Glowacki, J. Goldstein, H.F. Heath, M.-L. Holmberg, L. Kreczko, S. Paramesvaran, L. Robertshaw, S. Seif El Nasr-Storey, V.J. Smith, N. Stylianou [76], K. Walkingshaw Pass

University of Bristol, Bristol, United Kingdom

A.H. Ball, K.W. Bell, A. Belyaev [77], C. Brew, R.M. Brown, D.J.A. Cockerill, C. Cooke, A. Elliot, K.V. Ellis, K. Harder, S. Harper, J. Linacre, K. Manolopoulos, D.M. Newbold, E. Olaiya, D. Petyt, T. Reis, A.R. Sahasransu, G. Salvi, T. Schuh, C.H. Shepherd-Themistocleous, I.R. Tomalin, K.C. Whalen, T. Williams

Rutherford Appleton Laboratory, Didcot, United Kingdom

I. Andreou, R. Bainbridge, P. Bloch, C.E. Brown, O. Buchmuller, V. Cacchio, C.A. Carrillo Montoya, G.S. Chahal [78], D. Colling, J.S. Dancu, I. Das, P. Dauncey, G. Davies, J. Davies, M. Della Negra, S. Fayer, G. Fedi, G. Hall, M.H. Hassanshahi, A. Howard, G. Iles, M. Knight, J. Langford, J. León Holgado, L. Lyons, A.-M. Magnan, S. Mallios, M. Mieskolainen, J. Nash [79], M. Pesaresi, P.B. Pradeep, B.C. Radburn-Smith, A. Richards, A. Rose, K. Savva, C. Seez, R. Shukla, A. Tapper, K. Uchida, G.P. Uttley, L.H. Vage, T. Virdee [29], M. Vojinovic, N. Wardle, D. Winterbottom

Imperial College, London, United Kingdom

K. Coldham, J.E. Cole, A. Khan, P. Kyberd, I.D. Reid

Brunel University, Uxbridge, United Kingdom

S. Abdullin, A. Brinkerhoff, E. Collins, J. Dittmann, K. Hatakeyama, J. Hiltbrand, B. McMaster, J. Samudio, S. Sawant, C. Sutantawibul, J. Wilson

Baylor University, Waco, TX, USA

R. Bartek, A. Dominguez, C. Huerta Escamilla, A.E. Simsek, R. Uniyal, A.M. Vargas Hernandez

Catholic University of America, Washington, DC, USA

B. Bam, A. Buchot Perraguin, R. Chudasama, S.I. Cooper, C. Crovella, S.V. Gleyzer, E. Pearson, C.U. Perez, P. Rumerio [80], E. Usai, R. Yi

The University of Alabama, Tuscaloosa, AL, USA

A. Akpinar, C. Cosby, G. De Castro, Z. Demiragli, C. Erice, C. Fangmeier, C. Fernandez Madrazo, E. Fontanesi, D. Gastler, F. Golf, S. Jeon, J. O'cain, I. Reed, J. Rohlf, K. Salyer, D. Sperka, D. Spitzbart, I. Suarez, A. Tsatsos, A.G. Zecchinelli

Boston University, Boston, MA, USA

G. Benelli, D. Cutts, L. Gouskos, M. Hadley, U. Heintz, J.M. Hogan [81], T. Kwon, G. Landsberg, K.T. Lau, D. Li, J. Luo, S. Mondal, M. Narain [†], N. Pervan, T. Russell, S. Sagir [82], F. Simpson, M. Stamenkovic, N. Venkatasubramanian, X. Yan

Brown University, Providence, RI, USA

S. Abbott, C. Brainerd, R. Breedon, H. Cai, M. Calderon De La Barca Sanchez, M. Chertok, M. Citron, J. Conway, P.T. Cox, R. Erbacher, F. Jensen, O. Kukral, G. Mocellin, M. Mulhearn, S. Ostrom, W. Wei, Y. Yao, S. Yoo, F. Zhang

University of California, Davis, Davis, CA, USA

M. Bachtis, R. Cousins, A. Datta, G. Flores Avila, J. Hauser, M. Ignatenko, M.A. Iqbal, T. Lam, E. Manca, A. Nunez Del Prado, D. Saltzberg, V. Valuev

University of California, Los Angeles, CA, USA

R. Clare, J.W. Gary, M. Gordon, G. Hanson, W. Si

University of California, Riverside, Riverside, CA, USA

A. Aportela, A. Arora, J.G. Branson, S. Cittolin, S. Cooperstein, D. Diaz, J. Duarte, L. Giannini, Y. Gu, J. Guiang, R. Kansal, V. Krutelyov, R. Lee, J. Letts, M. Masciovecchio, F. Mokhtar, S. Mukherjee, M. Pieri, M. Quinnan, B.V. Sathia Narayanan, V. Sharma, M. Tadel, E. Vourliotis, F. Würthwein, Y. Xiang, A. Yagil

University of California, San Diego, La Jolla, CA, USA

A. Barzdukas, L. Brennan, C. Campagnari, K. Downham, C. Grieco, J. Incandela, J. Kim, A.J. Li, P. Masterson, H. Mei, J. Richman, S.N. Santpur, U. Sarica, R. Schmitz, F. Setti, J. Sheplock, D. Stuart, T.Á. Vámi, S. Wang, D. Zhang

University of California, Santa Barbara - Department of Physics, Santa Barbara, CA, USA

A. Bornheim, O. Cerri, A. Latorre, J. Mao, H.B. Newman, G. Reales Gutiérrez, M. Spiropulu, J.R. Vlimant, C. Wang, S. Xie, R.Y. Zhu

California Institute of Technology, Pasadena, CA, USA

J. Alison, S. An, P. Bryant, M. Cremonesi, V. Dutta, T. Ferguson, T.A. Gómez Espinosa, A. Harilal, A. Kallil Tharayil, C. Liu, T. Mudholkar, S. Murthy, P. Palit, K. Park, M. Paulini, A. Roberts, A. Sanchez, W. Terrill

Carnegie Mellon University, Pittsburgh, PA, USA

J.P. Cumalat, W.T. Ford, A. Hart, A. Hassani, G. Karathanasis, N. Manganelli, A. Perloff, C. Savard, N. Schonbeck, K. Stenson, K.A. Ulmer, S.R. Wagner, N. Zipper, D. Zuolo

University of Colorado Boulder, Boulder, CO, USA

J. Alexander, S. Bright-Thonney, X. Chen, D.J. Cranshaw, J. Fan, X. Fan, S. Hogan, P. Kotamnives, J. Monroy, M. Oshiro, J.R. Patterson, M. Reid, A. Ryd, J. Thom, P. Wittich, R. Zou

Cornell University, Ithaca, NY, USA

M. Albrow, M. Alyari, O. Amram, G. Apollinari, A. Apresyan, L.A.T. Bauerdick, D. Berry, J. Berryhill, P.C. Bhat, K. Burkett, J.N. Butler, A. Canepa, G.B. Cerati, H.W.K. Cheung, F. Chlebana, G. Cummings, J. Dickinson, I. Dutta, V.D. Elvira, Y. Feng, J. Freeman, A. Gandrakota, Z. Gecse, L. Gray, D. Green, A. Grummer, S. Grünendahl, D. Guerrero, O. Gutsche, R.M. Harris, R. Heller, T.C. Herwig, J. Hirschauer, B. Jayatilaka, S. Jindariani, M. Johnson, U. Joshi, T. Klijnsma, B. Klima, K.H.M. Kwok, S. Lammel, D. Lincoln, R. Lipton, T. Liu, C. Madrid, K. Maeshima, C. Mantilla, D. Mason, P. McBride, P. Merkel, S. Mrenna, S. Nahn, J. Ngadiuba, D. Noonan, S. Norberg, V. Papadimitriou, N. Pastika,

K. Pedro, C. Pena[83], F. Ravera, A. Reinsvold Hall[84], L. Ristori, M. Safdari, E. Sexton-Kennedy, N. Smith, A. Soha, L. Spiegel, S. Stoynev, J. Strait, L. Taylor, S. Tkaczyk, N.V. Tran, L. Uplegger, E.W. Vaandering, I. Zoi

Fermi National Accelerator Laboratory, Batavia, IL, USA

C. Aruta, P. Avery, D. Bourilkov, P. Chang, V. Cherepanov, R.D. Field, E. Koenig, M. Kolosova, J. Konigsberg, A. Korytov, K. Matchev, N. Menendez, G. Mitselmakher, K. Mohrman, A. Muthirakalayil Madhu, N. Rawal, S. Rosenzweig, Y. Takahashi, J. Wang

University of Florida, Gainesville, FL, USA

T. Adams, A. Al Kadhim, A. Askew, S. Bower, R. Habibullah, V. Hagopian, R. Hashmi, R.S. Kim, S. Kim, T. Kolberg, G. Martinez, H. Prosper, P.R. Prova, M. Wulansatiti, R. Yohay, J. Zhang

Florida State University, Tallahassee, FL, USA

B. Alsufyani, M.M. Baarmand, S. Butalla, S. Das, T. Elkafrawy[85], M. Hohlmann, M. Rahmani, E. Yanes

Florida Institute of Technology, Melbourne, FL, USA

M.R. Adams, A. Baty, C. Bennett, R. Cavanaugh, R. Escobar Franco, O. Evdokimov, C.E. Gerber, M. Hawksworth, A. Hingrajiya, D.J. Hofman, J.h. Lee, D.S. Lemos, A.H. Merrit, C. Mills, S. Nanda, G. Oh, B. Ozek, D. Pilipovic, R. Pradhan, E. Prifti, T. Roy, S. Rudrabhatla, M.B. Tonjes, N. Varelas, M.A. Wadud, Z. Ye, J. Yoo

University of Illinois Chicago, Chicago, USA

M. Alhusseini, D. Blend, K. Dilsiz[86], L. Emediato, G. Karaman, O.K. Köseyan, J.-P. Merlo, A. Mestvirishvili[87], O. Neogi, H. Ogul[88], Y. Onel, A. Penzo, C. Snyder, E. Tiras[89]

The University of Iowa, Iowa City, IA, USA

B. Blumenfeld, L. Corcodilos, J. Davis, A.V. Gritsan, L. Kang, S. Kyriacou, P. Maksimovic, M. Roguljic, J. Roskes, S. Sekhar, M. Swartz

Johns Hopkins University, Baltimore, MD, USA

A. Abreu, L.F. Alcerro Alcerro, J. Anguiano, S. Arteaga Escatel, P. Baringer, A. Bean, Z. Flowers, D. Grove, J. King, G. Krintiras, M. Lazarovits, C. Le Mahieu, J. Marquez, M. Murray, M. Nickel, M. Pitt, S. Popescu[90], C. Rogan, C. Royon, R. Salvatico, S. Sanders, C. Smith, G. Wilson

The University of Kansas, Lawrence, KS, USA

B. Allmond, R. Gujju Gurunadha, A. Ivanov, K. Kaadze, Y. Maravin, J. Natoli, D. Roy, G. Sorrentino

Kansas State University, Manhattan, KS, USA

A. Baden, A. Belloni, J. Bistany-riebman, Y.M. Chen, S.C. Eno, N.J. Hadley, S. Jabeen, R.G. Kellogg, T. Koeth, B. Kronheim, Y. Lai, S. Lascio, A.C. Mignerey, S. Nabili, C. Palmer, C. Papageorgakis, M.M. Paranjpe, L. Wang

University of Maryland, College Park, MD, USA

J. Bendavid, I.A. Cali, P.c. Chou, M. D'Alfonso, J. Eysermans, C. Freer, G. Gomez-Ceballos, M. Goncharov, G. Grosso, P. Harris, D. Hoang, D. Kovalskyi, J. Krupa, L. Lavezzo, Y.-J. Lee,

K. Long, C. Mcginn, A. Novak, C. Paus, C. Roland, G. Roland, S. Rothman, G.S.F. Stephans, Z. Wang, B. Wyslouch, T.J. Yang

Massachusetts Institute of Technology, Cambridge, MA, USA

B. Crossman, B.M. Joshi, C. Kapsiak, M. Krohn, D. Mahon, J. Mans, B. Marzocchi, R. Rusack, R. Saradhy, N. Strobbe

University of Minnesota, Minneapolis, MN, USA

K. Bloom, D.R. Claes, G. Haza, J. Hossain, C. Joo, I. Kravchenko, J.E. Siado, W. Tabb, A. Vagnerini, A. Wightman, F. Yan, D. Yu

University of Nebraska-Lincoln, Lincoln, NE, USA

H. Bandyopadhyay, L. Hay, H.w. Hsia, I. Iashvili, A. Kalogeropoulos, A. Kharchilava, M. Morris, D. Nguyen, S. Rappoccio, H. Rejeb Sfar, A. Williams, P. Young

State University of New York at Buffalo, Buffalo, NY, USA

G. Alverson, E. Barberis, J. Bonilla, J. Dervan, Y. Haddad, Y. Han, A. Krishna, J. Li, M. Lu, G. Madigan, R. Mccarthy, D.M. Morse, V. Nguyen, T. Orimoto, A. Parker, L. Skinnari, D. Wood

Northeastern University, Boston, MA, USA

J. Bueghly, S. Dittmer, K.A. Hahn, Y. Liu, Y. Miao, D.G. Monk, M.H. Schmitt, A. Taliercio, M. Velasco

Northwestern University, Evanston, IL, USA

G. Agarwal, R. Band, R. Bucci, S. Castells, A. Das, R. Goldouzian, M. Hildreth, K.W. Ho, K. Hurtado Anampa, T. Ivanov, C. Jessop, K. Lannon, J. Lawrence, N. Loukas, L. Lutton, J. Mariano, N. Marinelli, I. Mcalister, T. McCauley, C. Mcgrady, C. Moore, Y. Musienko[17], H. Nelson, M. Osherson, A. Piccinelli, R. Ruchti, A. Townsend, Y. Wan, M. Wayne, H. Yockey, M. Zarucki, L. Zygala

University of Notre Dame, Notre Dame, IN, USA

A. Basnet, B. Bylsma, M. Carrigan, L.S. Durkin, C. Hill, M. Joyce, M. Nunez Ornelas, K. Wei, B.L. Winer, B.R. Yates

The Ohio State University, Columbus, OH, USA

H. Bouchamaoui, P. Das, G. Dezoort, P. Elmer, A. Frankenthal, B. Greenberg, N. Haubrich, K. Kennedy, G. Kopp, S. Kwan, D. Lange, A. Loeliger, D. Marlow, I. Ojalvo, J. Olsen, A. Shevelev, D. Stickland, C. Tully

Princeton University, Princeton, NJ, USA

S. Malik

University of Puerto Rico, Mayaguez, PR, USA

A.S. Bakshi, S. Chandra, R. Chawla, A. Gu, L. Gutay, M. Jones, A.W. Jung, A.M. Koshy, M. Liu, G. Negro, N. Neumeister, G. Paspalaki, S. Piperov, V. Scheurer, J.F. Schulte, M. Stojanovic, J. Thieman, A.K. Virdi, F. Wang, W. Xie

Purdue University, West Lafayette, IN, USA

J. Dolen, N. Parashar, A. Pathak

Purdue University Northwest, Hammond, IN, USA

D. Acosta, T. Carnahan, K.M. Ecklund, P.J. Fernández Manteca, S. Freed, P. Gardner, F.J.M. Geurts, W. Li, J. Lin, O. Miguel Colin, B.P. Padley, R. Redjimi, J. Rotter, E. Yigitbasi, Y. Zhang

Rice University, Houston, TX, USA

A. Bodek, P. de Barbaro, R. Demina, J.L. Dulemba, A. Garcia-Bellido, O. Hindrichs, A. Khukhunaishvili, N. Parmar, P. Parygin[91], E. Popova[91], R. Taus

University of Rochester, Rochester, NY, USA

B. Chiarito, J.P. Chou, S.V. Clark, D. Gadkari, Y. Gershtein, E. Halkiadakis, M. Heindl, C. Houghton, D. Jaroslawski, S. Konstantinou, I. Laflotte, A. Lath, R. Montalvo, K. Nash, J. Reichert, H. Routray, P. Saha, S. Salur, S. Schnetzer, S. Somalwar, R. Stone, S.A. Thayil, S. Thomas, J. Vora, H. Wang

Rutgers, The State University of New Jersey, Piscataway, NJ, USA

D. Ally, A.G. Delannoy, S. Fiorendi, S. Higginbotham, T. Holmes, A.R. Kanuganti, N. Karunarathna, L. Lee, E. Nibigira, S. Spanier

University of Tennessee, Knoxville, TN, USA

D. Aebi, M. Ahmad, T. Akhter, O. Bouhali[92], R. Eusebi, J. Gilmore, T. Huang, T. Kamon[93], H. Kim, S. Luo, R. Mueller, D. Overton, D. Rathjens, A. Safonov

Texas A&M University, College Station, TX, USA

N. Akchurin, J. Damgov, N. Gogate, V. Hegde, A. Hussain, Y. Kazhykarim, K. Lamichhane, S.W. Lee, A. Mankel, T. Peltola, I. Volobouev

Texas Tech University, Lubbock, TX, USA

E. Appelt, Y. Chen, S. Greene, A. Gurrola, W. Johns, R. Kunnawalkam Elayavalli, A. Melo, F. Romeo, P. Sheldon, S. Tuo, J. Velkovska, J. Viinikainen

Vanderbilt University, Nashville, TN, USA

B. Cardwell, B. Cox, J. Hakala, R. Hirosky, A. Ledovskoy, C. Neu

University of Virginia, Charlottesville, VA, USA

S. Bhattacharya, P.E. Karchin

Wayne State University, Detroit, MI, USA

A. Aravind, S. Banerjee, K. Black, T. Bose, S. Dasu, I. De Bruyn, P. Everaerts, C. Galloni, H. He, M. Herndon, A. Herve, C.K. Koraka, A. Lanaro, R. Loveless, J. Madhusudanan Sreekala, A. Mallampalli, A. Mohammadi, S. Mondal, G. Parida, L. Pétré, D. Pinna, A. Savin, V. Shang, V. Sharma, W.H. Smith, D. Teague, H.F. Tsoi, W. Vetens, A. Warden

University of Wisconsin - Madison, Madison, WI, USA

S. Afanasiev, V. Alexakhin, V. Andreev, Yu. Andreev, T. Aushev, M. Azarkin, A. Babaev, V. Blinov[94], E. Boos, V. Borshch, D. Budkouski, V. Bunichev, V. Chekhovsky, R. Chistov[94], M. Danilov[94], A. Dermenev, T. Dimova[94], D. Druzhkin[95], M. Dubinin[83], L. Dudko, A. Ershov, G. Gavrilov, V. Gavrilov, S. Gninenko, V. Golovtcov, N. Golubev, I. Golutvin[†], I. Gorbunov, A. Gribushin, Y. Ivanov, V. Kachanov, V. Karjavine, A. Karneyeu, V. Kim[94], M. Kirakosyan, D. Kirpichnikov, M. Kirsanov, V. Klyukhin, O. Kodolova[96], D. Konstantinov, V. Korenkov, A. Kozyrev[94], N. Krasnikov, A. Lanev, P. Levchenko[97], N. Lychkovskaya, V. Makarenko, A. Malakhov, V. Matveev[94], V. Murzin, A. Nikitenko[98,96], S. Obraztsov, V. Oreshkin,

V. Palichik, V. Perelygin, S. Petrushanko, S. Polikarpov[94], V. Popov, O. Radchenko[94], M. Savina, V. Savrin, V. Shalaev, S. Shmatov, S. Shulha, Y. Skovpen[94], S. Slabospitskii, V. Smirnov, A. Snigirev, D. Sosnov, V. Sulimov, A. Terkulov, O. Teryaev, I. Tlisova, A. Toropin, L. Uvarov, A. Uzunian, A. Vorobyev[†], N. Voytishin, B.S. Yuldashev[99], A. Zarubin, I. Zhizhin, A. Zhokin

Authors affiliated with an institute or an international laboratory covered by a cooperation agreement with CERN

[†] Deceased.
[1] Also at Yerevan State University, Yerevan, Armenia.
[2] Also at TU Wien, Vienna, Austria.
[3] Also at Institute of Basic and Applied Sciences, Faculty of Engineering, Arab Academy for Science, Technology and Maritime Transport, Alexandria, Egypt.
[4] Also at Ghent University, Ghent, Belgium.
[5] Also at Universidade do Estado do Rio de Janeiro, Rio de Janeiro, Brazil.
[6] Also at Universidade Estadual de Campinas, Campinas, Brazil.
[7] Also at Federal University of Rio Grande do Sul, Porto Alegre, Brazil.
[8] Also at UFMS, Nova Andradina, Brazil.
[9] Also at Nanjing Normal University, Nanjing, China.
[10] Now at The University of Iowa, Iowa City, Iowa, USA.
[11] Also at University of Chinese Academy of Sciences, Beijing, China.
[12] Also at China Center of Advanced Science and Technology, Beijing, China.
[13] Also at University of Chinese Academy of Sciences, Beijing, China.
[14] Also at China Spallation Neutron Source, Guangdong, China.
[15] Now at Henan Normal University, Xinxiang, China.
[16] Also at Université Libre de Bruxelles, Bruxelles, Belgium.
[17] Also at an institute or an international laboratory covered by a cooperation agreement with CERN.
[18] Also at Suez University, Suez, Egypt.
[19] Now at British University in Egypt, Cairo, Egypt.
[20] Also at Purdue University, West Lafayette, Indiana, USA.
[21] Also at Université de Haute Alsace, Mulhouse, France.
[22] Also at Istinye University, Istanbul, Turkey.
[23] Also at The University of the State of Amazonas, Manaus, Brazil.
[24] Also at University of Hamburg, Hamburg, Germany.
[25] Also at RWTH Aachen University, III. Physikalisches Institut A, Aachen, Germany.
[26] Also at Bergische University Wuppertal (BUW), Wuppertal, Germany.
[27] Also at Brandenburg University of Technology, Cottbus, Germany.
[28] Also at Forschungszentrum Jülich, Juelich, Germany.
[29] Also at CERN, European Organization for Nuclear Research, Geneva, Switzerland.
[30] Also at Institute of Nuclear Research ATOMKI, Debrecen, Hungary.
[31] Now at Universitatea Babes-Bolyai - Facultatea de Fizica, Cluj-Napoca, Romania.
[32] Also at MTA-ELTE Lendület CMS Particle and Nuclear Physics Group, Eötvös Loránd University, Budapest, Hungary.
[33] Also at HUN-REN Wigner Research Centre for Physics, Budapest, Hungary.
[34] Also at Physics Department, Faculty of Science, Assiut University, Assiut, Egypt.
[35] Also at Punjab Agricultural University, Ludhiana, India.
[36] Also at University of Visva-Bharati, Santiniketan, India.
[37] Also at Indian Institute of Science (IISc), Bangalore, India.
[38] Also at IIT Bhubaneswar, Bhubaneswar, India.
[39] Also at Institute of Physics, Bhubaneswar, India.
[40] Also at University of Hyderabad, Hyderabad, India.
[41] Also at Deutsches Elektronen-Synchrotron, Hamburg, Germany.
[42] Also at Isfahan University of Technology, Isfahan, Iran.
[43] Also at Sharif University of Technology, Tehran, Iran.
[44] Also at Department of Physics, University of Science and Technology of Mazandaran, Behshahr, Iran.
[45] Also at Department of Physics, Isfahan University of Technology, Isfahan, Iran.
[46] Also at Department of Physics, Faculty of Science, Arak University, ARAK, Iran.
[47] Also at Helwan University, Cairo, Egypt.
[48] Also at Italian National Agency for New Technologies, Energy and Sustainable Economic Development, Bologna, Italy.
[49] Also at Centro Siciliano di Fisica Nucleare e di Struttura Della Materia, Catania, Italy.
[50] Also at Università degli Studi Guglielmo Marconi, Roma, Italy.
[51] Also at Scuola Superiore Meridionale, Università di Napoli 'Federico II', Napoli, Italy.
[52] Also at Fermi National Accelerator Laboratory, Batavia, Illinois, USA.
[53] Also at Consiglio Nazionale delle Ricerche - Istituto Officina dei Materiali, Perugia, Italy.
[54] Also at Department of Applied Physics, Faculty of Science and Technology, Universiti Kebangsaan Malaysia, Bangi, Malaysia.
[55] Also at Consejo Nacional de Ciencia y Tecnología, Mexico City, Mexico.
[56] Also at Trincomalee Campus, Eastern University, Sri Lanka, Nilaveli, Sri Lanka.
[57] Also at Saegis Campus, Nugegoda, Sri Lanka.
[58] Also at National and Kapodistrian University of Athens, Athens, Greece.
[59] Also at Ecole Polytechnique Fédérale Lausanne, Lausanne, Switzerland.
[60] Also at Universität Zürich, Zurich, Switzerland.
[61] Also at Stefan Meyer Institute for Subatomic Physics, Vienna, Austria.
[62] Also at Laboratoire d'Annecy-le-Vieux de Physique des Particules, IN2P3-CNRS, Annecy-le-Vieux, France.
[63] Also at Near East University, Research Center of Experimental Health Science, Mersin, Turkey.
[64] Also at Konya Technical University, Konya, Turkey.
[65] Also at Izmir Bakircay University, Izmir, Turkey.
[66] Also at Adiyaman University, Adiyaman, Turkey.

[67] Also at Bozok Universitetesi Rektörlügü, Yozgat, Turkey.
[68] Also at Marmara University, Istanbul, Turkey.
[69] Also at Milli Savunma University, Istanbul, Turkey.
[70] Also at Kafkas University, Kars, Turkey.
[71] Now at Istanbul Okan University, Istanbul, Turkey.
[72] Also at Hacettepe University, Ankara, Turkey.
[73] Also at Erzincan Binali Yildirim University, Erzincan, Turkey.
[74] Also at Istanbul University - Cerrahpasa, Faculty of Engineering, Istanbul, Turkey.
[75] Also at Yildiz Technical University, Istanbul, Turkey.
[76] Also at Vrije Universiteit Brussel, Brussel, Belgium.
[77] Also at School of Physics and Astronomy, University of Southampton, Southampton, United Kingdom.
[78] Also at IPPP Durham University, Durham, United Kingdom.
[79] Also at Monash University, Faculty of Science, Clayton, Australia.
[80] Also at Università di Torino, Torino, Italy.
[81] Also at Bethel University, St. Paul, Minnesota, USA.
[82] Also at Karamanoğlu Mehmetbey University, Karaman, Turkey.
[83] Also at California Institute of Technology, Pasadena, California, USA.
[84] Also at United States Naval Academy, Annapolis, Maryland, USA.
[85] Also at Ain Shams University, Cairo, Egypt.
[86] Also at Bingol University, Bingol, Turkey.
[87] Also at Georgian Technical University, Tbilisi, Georgia.
[88] Also at Sinop University, Sinop, Turkey.
[89] Also at Erciyes University, Kayseri, Turkey.
[90] Also at Horia Hulubei National Institute of Physics and Nuclear Engineering (IFIN-HH), Bucharest, Romania.
[91] Now at an institute or an international laboratory covered by a cooperation agreement with CERN.
[92] Also at Texas A&M University at Qatar, Doha, Qatar.
[93] Also at Kyungpook National University, Daegu, Korea.
[94] Also at another institute or international laboratory covered by a cooperation agreement with CERN.
[95] Also at Universiteit Antwerpen, Antwerpen, Belgium.
[96] Also at Yerevan Physics Institute, Yerevan, Armenia.
[97] Also at Northeastern University, Boston, Massachusetts, USA.
[98] Also at Imperial College, London, United Kingdom.
[99] Also at Institute of Nuclear Physics of the Uzbekistan Academy of Sciences, Tashkent, Uzbekistan.